2016 Spring

“Advanced Physical Metallurgy”

- Bulk Metallic Glasses -

04.06.2016

Eun Soo Park

Office: 33-313
Telephone: 880-7221
Email: espark@snu.ac.kr
Office hours: by appointment

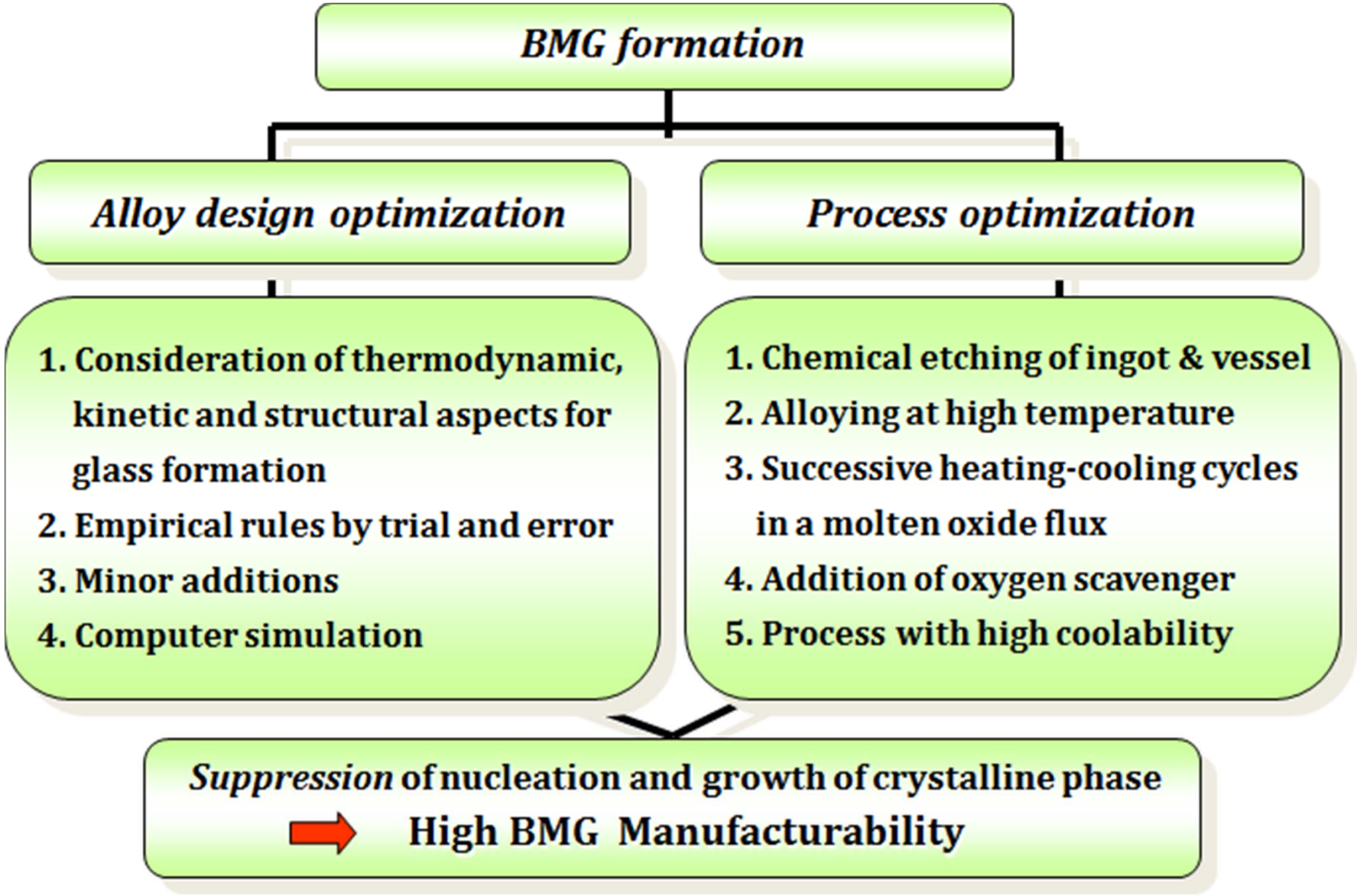
BMG formation
Alloy design optimization
Process optimization
1. Consideration of thermodynamic, kinetic and structural aspects for glass formation
2. Empirical rules by trial and error
3. Minor additions
4. Computer simulation
1. Chemical etching of ingot & vessel
2. Alloying at high temperature
3. Successive heating-cooling cycles in a molten oxide flux
4. Addition of oxygen scavenger
5. Process with high coolability
Suppression of nucleation and growth of crystalline phase
High BMG Manufacturability

Recent BMGs with critical size ≥ 10 mm

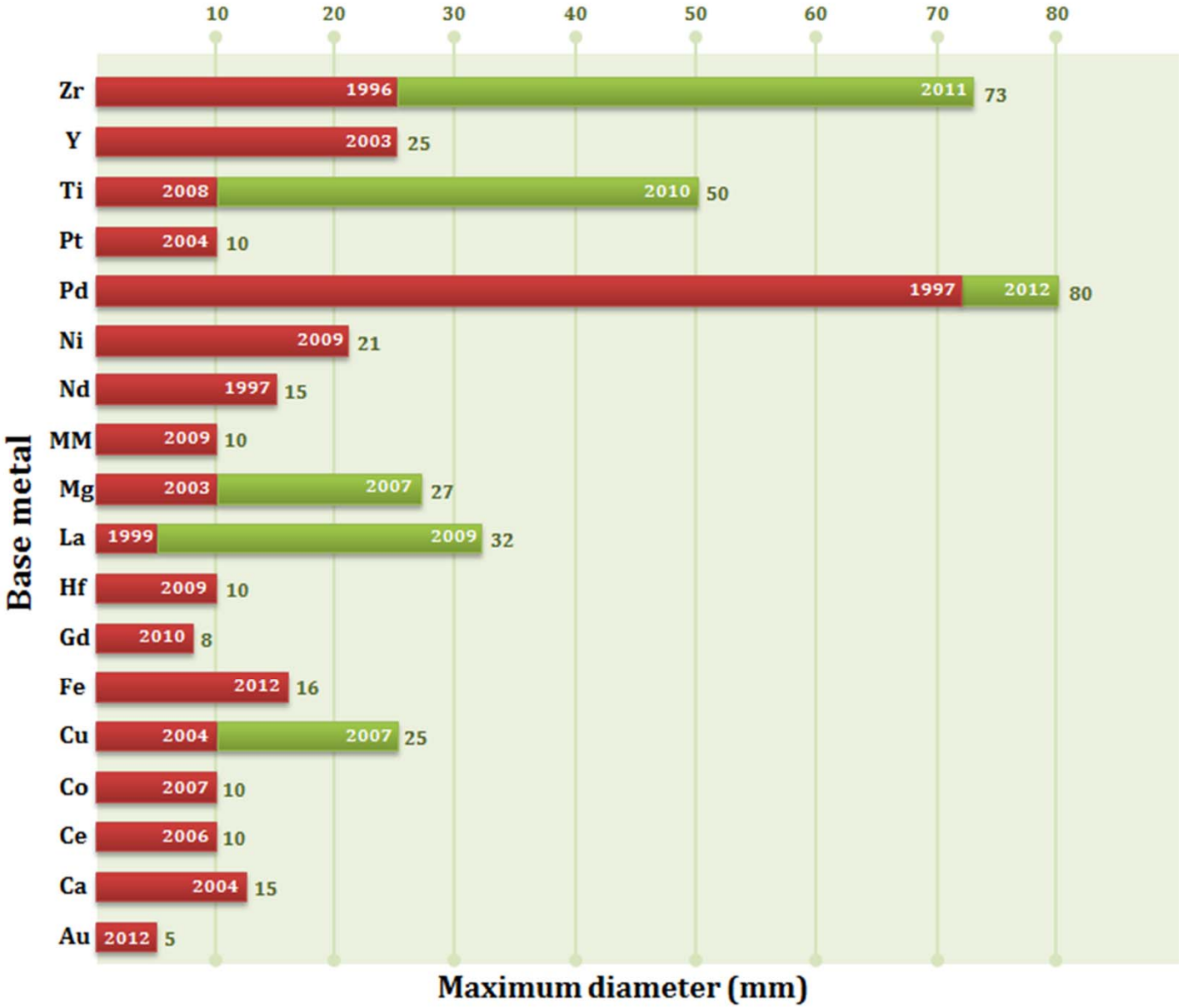

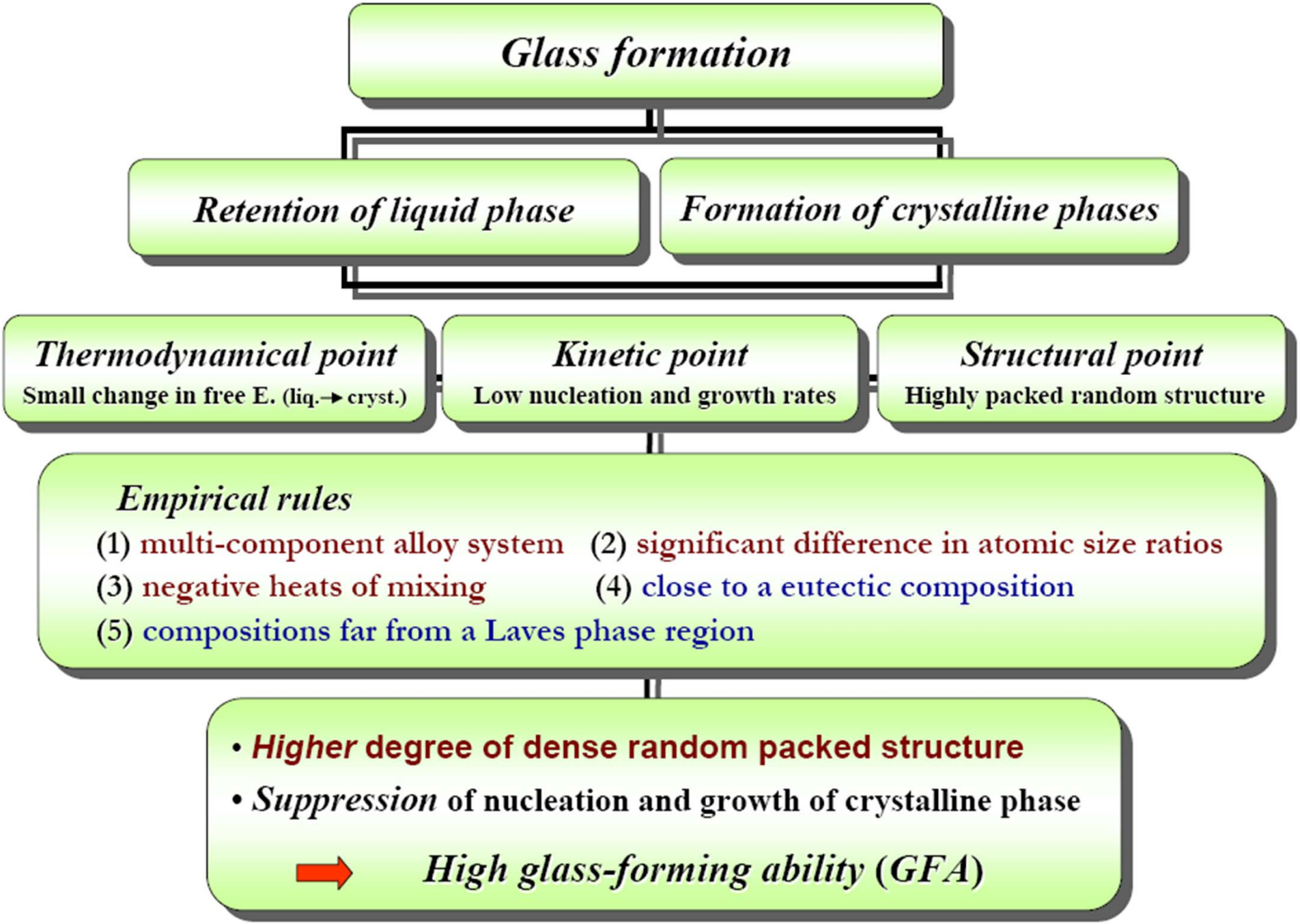
Glass formation
Retention of liquid phase
Formation of crystalline phases
Thermodynamical point
Small change in free E. (liq.→cryst.)
Kinetic point
Low nucleation and growth rates
Structural point
Highly packed random structure
Empirical rules
(1) multi-component alloy system
(2) significant difference in atomic size ratios
(3) negative heats of mixing
(4) close to a eutectic composition
(5) compositions far from a Laves phase region
• Higher degree of dense random packed structure
• Suppression of nucleation and growth of crystalline phase
High glass-forming ability (GFA)

Composites & Glass forming composition

< Symmetric Eutectic>

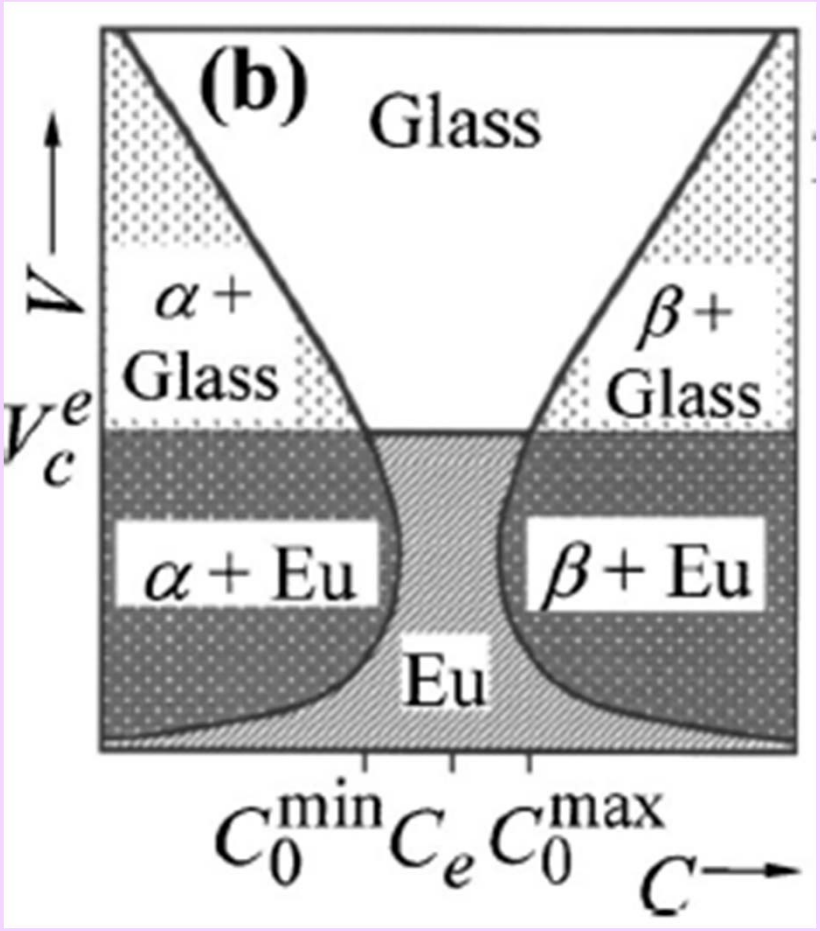

< Non-symmetric Eutectic>

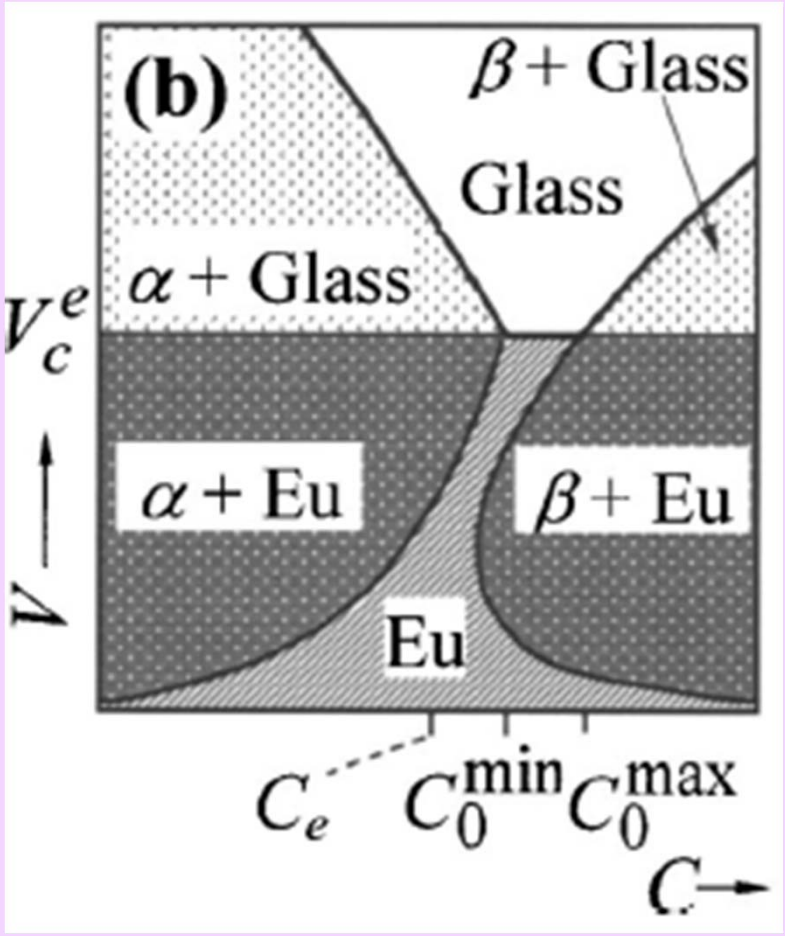

- Glass region is located between composites with different 2nd phases.

⇨ Useful to find the composition with maximum GFA

3.5 Topological Model (Structural aspect for glass formation)

Metallic glasses produced by RSP methods in the form of thin ribbons have been traditionally classified into two groups, viz., metal–metalloid and metal–metal types. Structural models of the metal-metalloid-type metallic glasses have identified that the best composition to form a glass is one that contains about 80 at.% of the metal component and 20 at.% of the metalloid component. The actual glass composition ranges observed are 75–85 at.% of the metal and 15–25 at.% of the metalloid. As stated in Chapter 2, the 80 at.% of the metal can be either a single transition metal or a combination of transition metals or one or a combination of noble metals. Similarly, the 20 at.% of the metalloid content could be made up of just one component or a mixture of a number of components. In the case of metal-metal types, however, there is no such restriction on compositions. Metal-metal-type metallic glasses have been observed to form over a wide range of compositions, starting from as low as 9 at.% of solute. Some typical compositions in which metal-metal type glasses have been obtained are $Cu_{25–72.5}Zr_{27.5–75}$, $Fe_{89–91}Zr_{9–11}$, $Mg_{68–75}Zn_{25–32}$, $Nb_{55}Ir_{45}$, and $Ni_{58–67}Zr_{33–42}$ [65].

* Metallic glass : Randomly dense packed structure

1) Atomic size difference: TM – metalloid (M, ex) Boron)

→ M is located at interior of the tetrahedron of four metal atoms (TM_4M)

→ denser ⇨ by increasing resistivity of crystallization, GFA ⇧

→ Ex) Fe-B: tetrahedron with B on the center position

1) interstitial site, B= simple atomic topology

2) skeleton structure

3) bonding nature: close to covalent bonding

Irrespective of the actual size of the voids and whether the above model is valid or not, it is of interest to note that the metal-metalloid-type binary phase diagrams exhibit deep eutectics at around a composition of 15–25 at.% metalloid. Some typical examples are Fe–B (17 at.% B), Au–Si (18.6 at.% Si), and Pd–Si (17.2 at.% Si). Therefore, the concepts of deep eutectics and structural models also seem to converge in obtaining glasses in the (transition or noble) metal-metalloid types.

3.5.2. Egami and Waseda Criterion

One of the possible ways by which a crystalline metallic material can become glassy is by the introduction of lattice strain. The lattice strain introduced disturbs the crystal lattice and once a critical strain is exceeded, the crystal becomes destabilized and becomes glassy. In fact, Egami takes pains to state that "In general, alloying makes glass formation easier, not because alloying stabilizes a glass, but because it destabilizes a crystal" [72, p. 576]. Using the atomic scale elasticity theory, Egami and Waseda [73] calculated the atomic level stresses in the solid solution (the solute atoms are assumed to occupy the substitutional lattice sites in the solid solution) and the glassy phase. They observed that in a glass, neither the local stress fluctuations nor the total strain energy vary much with solute concentration, when normalized with respect to the elastic moduli. But, in a solid solution, the strain energy was observed to increase continuously and linearly with solute content. Thus, beyond a critical solute concentration, the glassy alloy becomes energetically more favorable than the corresponding crystalline lattice. From the vast literature available on the formation of binary metallic glasses obtained by RSP methods, the authors noted that a minimum solute concentration was necessary in a binary alloy system to obtain the stable glassy phase by RSP methods.

2) min. solute content, C_B^*: empirical rule

By Egami & Waseda: in A-B binary system

$$C_B^{min}\left|\frac{(v_B - v_A)}{v_A}\right| = C_B^{min}\left|\left(\frac{r_B}{r_A}\right)^3 - 1\right| \approx 0.1$$

ν: atomic volume
A: matrix, B: solute

minimum concentration of B for glass formation 존재

→ Inversely proportional to atomic volume mismatch

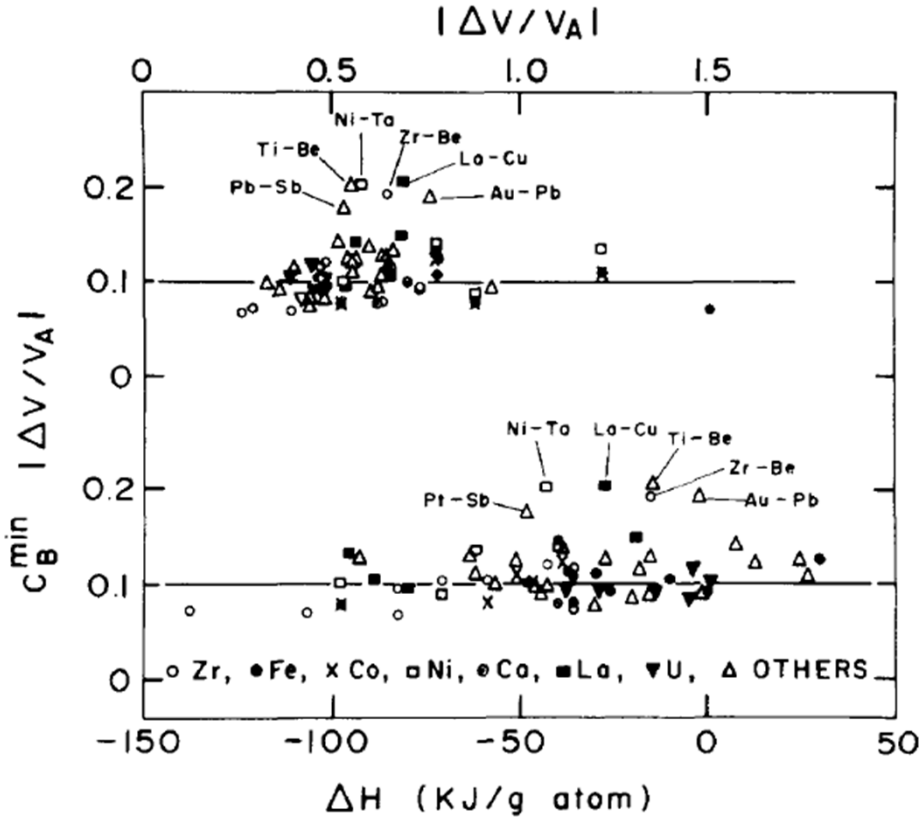

Fig. 1. Relation between $|\lambda_0| = C_B^{min}\,|\Delta v/v_A|$, and $|\Delta v/v_A|$ and ΔH, for 66 binary systems which can be vitrified by liquid quenching.

3.5.3. Nagel and Tauc Criterion

Nagel and Tauc [74,75] proposed that a glass is most likely to form if its electronic energy lies in a local metastable minimum with respect to composition change. They showed that if the structure factor corresponding to the first strong peak of the diffuse scattering curve, K_p, satisfies the relationship $K_p = 2\,k_F$, where k_F is the wave vector at the Fermi energy, then the electronic energy does indeed occupy a local minimum.

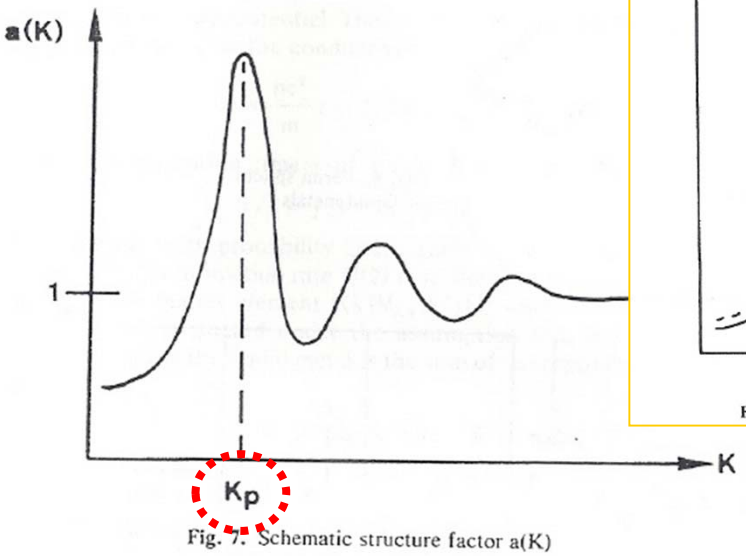

Fig. 7. Schematic structure factor a(K)

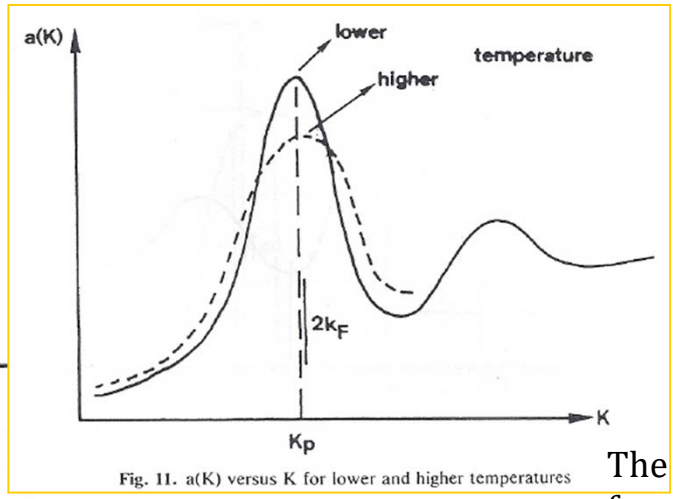

Fig. 11. a(K) versus K for lower and higher temperatures

$Kp = 2\,k_F$

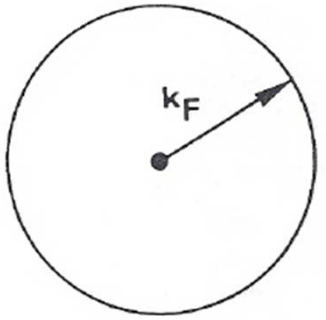

The conduction electrons are suppose to form a degenerate free-electron gas with a spherical Fermi surface.

$$2K_F = 2(3\pi^2 n)^{1/3} = 2\left(\frac{3\pi^2}{eR_H}\right)^{1/3}$$

a(K) Fourier transform of the pair correlation function g(r)

Kp Nearest neighbor distance of the liquid metal in K-space

: Diameter of Fermi surface

3.6 Bulk Metallic Glasses

Since 1989, intense research has been carried out in synthesizing and characterizing BMGs with a section thickness or diameter of a few millimeters to a few centimeters.

First, phase diagrams are not available for the multicomponent alloy systems.

Therefore, we do not know where the eutectic compositions lie, and much less about deep eutectics.

Additionally, because the number of components is really large, determining the minimum solute content will be a formidable problem since the contribution of each component to the volumetric strain is going to be different depending on their atomic sizes.

Therefore, newer criteria have been proposed to explain glass formation in BMGs in view of the large number of components present.

3.7 Inoue Criteria – Empirical Rules

1. The alloy must contain at least three components. The formation of glass becomes easier with increasing number of components in the alloy system.

a) Thermodynamic point of view

Since the value of ΔS_f can be significantly increased by increasing the number of components in the alloy, it has been relatively easy to produce BMGs in multicomponent alloys. Since an increase in ΔS_f also leads to an increase in the degree of the dense random packing of atoms, this results in a decrease in ΔH_f and also an increase in the solid–liquid interfacial energy, σ. Both these factors contribute to a decrease in the free energy of the system.

b) Kinetic point of view

Since the equation for homogeneous nucleation rate for the formation of crystalline nuclei from a supercooled melt (Equation 2.4) contains η, α, and β, control of these parameters can lead to a reduction in the nucleation rate. For example, a reduction in ΔH_f, and an increase in σ and/or ΔS_f can be achieved by an increase in α and β values. This, in turn, will decrease the nucleation rate and consequently promote glass formation. An increase in the viscosity of the melt will also lead to a reduction in both nucleation and growth rates.

3.7 Inoue Criteria – Empirical Rules

2. A significant atomic size difference should exist among the constituent elements in the alloy. It is suggested that the atomic size differences should be above about 12% among the main constituent elements.

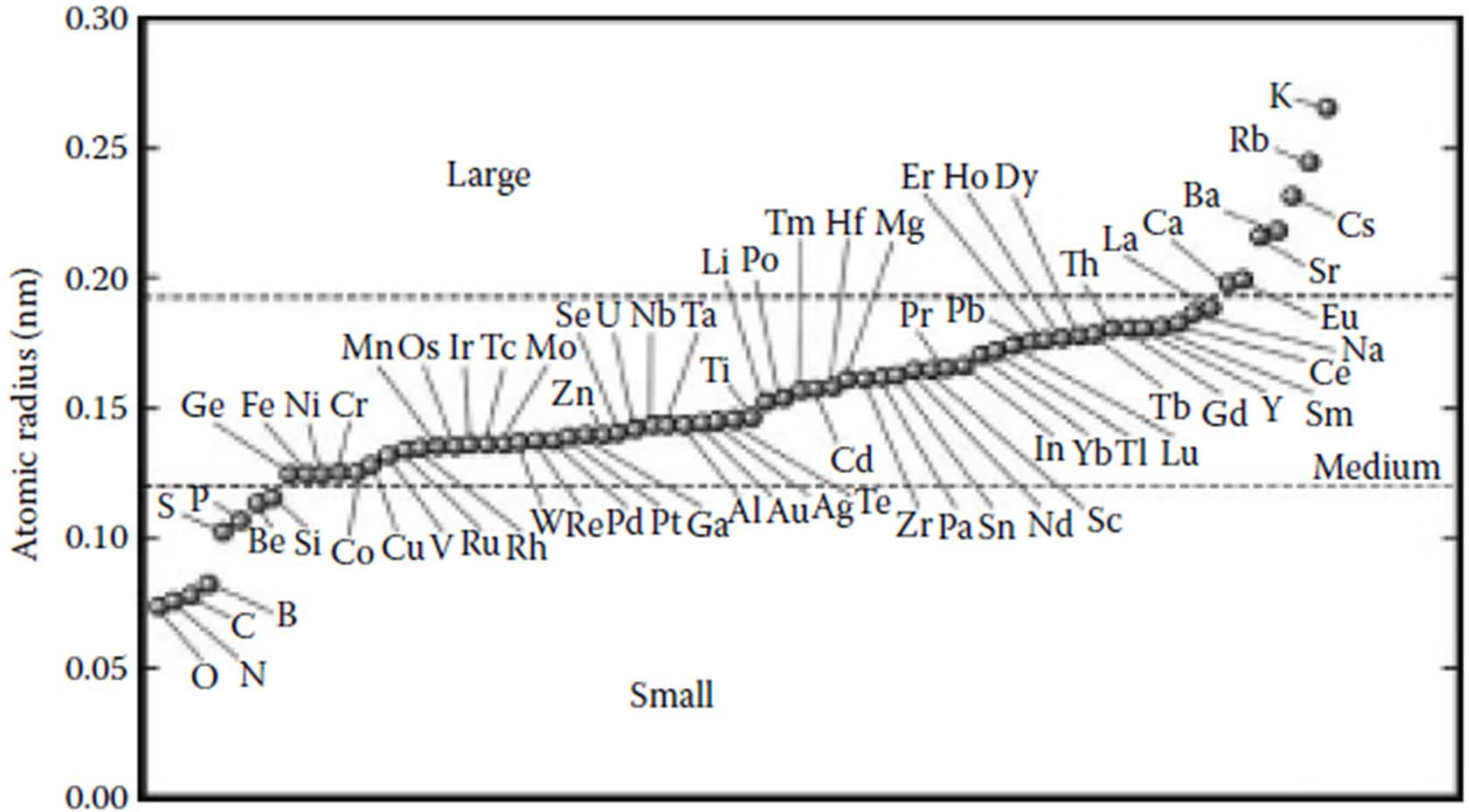

FIGURE 3.4
Atomic diameters of the elements that constitute bulk metallic glasses. These can be classified into three major groups of large, medium, and small sizes.

< significant difference in atomic size ratios >

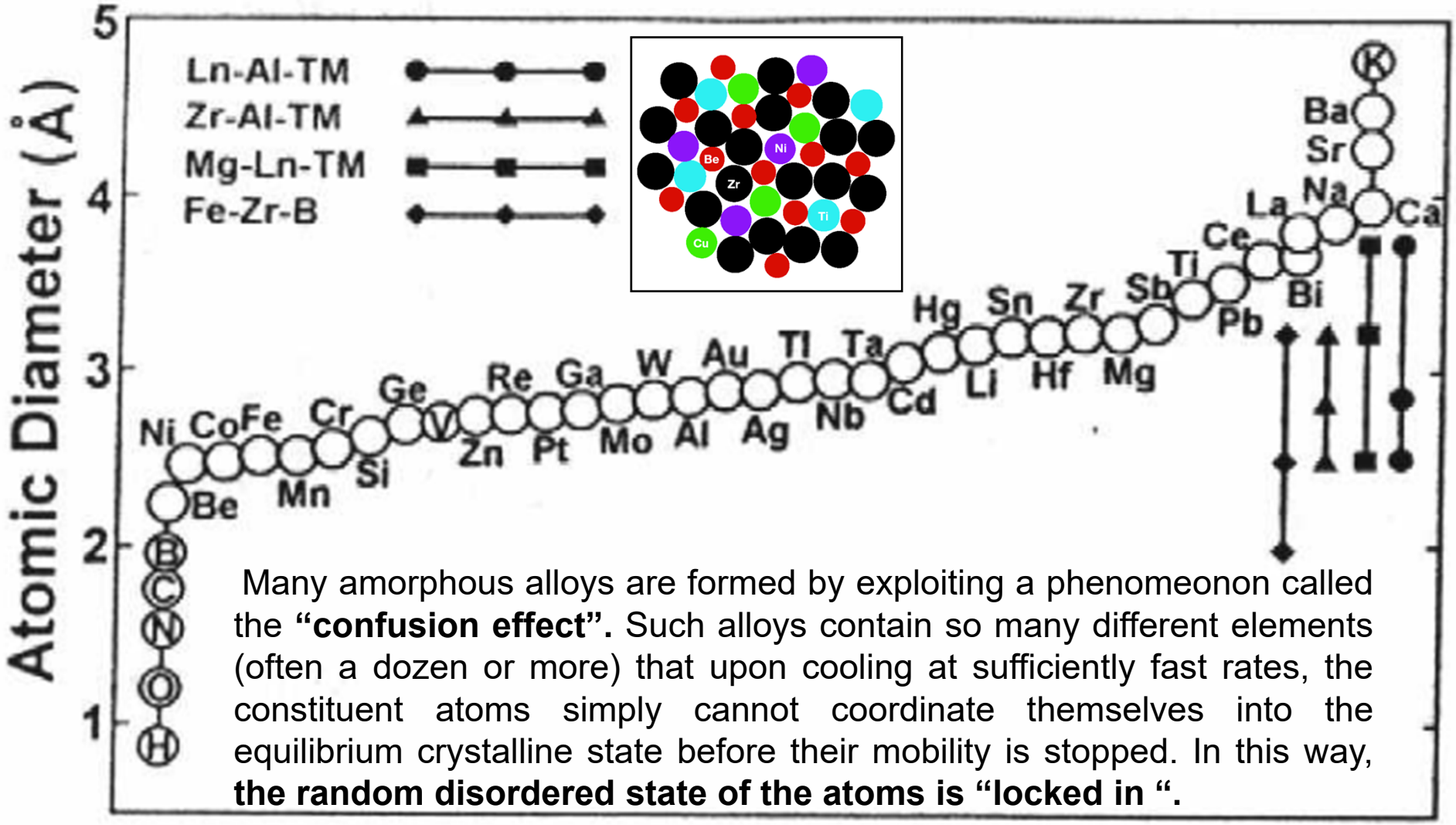

Many amorphous alloys are formed by exploiting a phenomeonon called the **"confusion effect".** Such alloys contain so many different elements (often a dozen or more) that upon cooling at sufficiently fast rates, the constituent atoms simply cannot coordinate themselves into the equilibrium crystalline state before their mobility is stopped. In this way, **the random disordered state of the atoms is "locked in ".**

3.7 Inoue Criteria – Empirical Rules

3. There should be negative heat of mixing among the (major) constituent elements in the alloy system.

The combination of the significant differences in atomic sizes between the constituent elements and the negative heat of mixing is expected to result in efficient packing of clusters (see Section 3.12.2) and consequently increase the density of random packing of atoms in the supercooled liquid state. This, in turn, leads to increased liquid–solid interfacial energy, σ and decreased atomic diffusivity, both contributing to enhanced glass formation.

Table 3.3

Nearest Neighbor Distances (r) and Coordination Numbers (N) of the Different Atomic Pairs in a Glassy $Zr_{60}Al_{15}Ni_{25}$ Alloy Both in the As-Quenched and Crystallized States

Condition		r_1 (nm)	N_{Zr-Ni}	r_2 (nm)	N_{Zr-Zr}	N_{Zr-Al}
As-quenched	(a)	0.267 ± 0.002	2.3 ± 0.2	0.317 ± 0.002	10.3 ± 0.7	−0.1 ± 0.9
	(b)	0.267 ± 0.002	2.1 ± 0.2	—	—	—
	(c)	0.269 ± 0.002	2.3 ± 0.2	—	—	—
Crystallized	(a)	0.268 ± 0.002	3.0 ± 0.2	0.322 ± 0.002	8.2 ± 0.7	0.8 ± 0.9
	(b)	0.267 ± 0.002	3.0 ± 0.2	—	—	—
	(c)	0.273 ± 0.002	2.3 ± 0.2	—	—	—

Source: Matsubara, E. et al., *Mater. Trans. JIM*, 33, 873, 1992. With permission.

Notes: Data from (a) ordinary radial distribution function (RDF), (b) conventional RDFs for Zr, and (c) conventional RDFs for Ni. "—" means that no values were given in the original publication.

Significant change in the coordination # of Zr-Al atomic pairs on crystallization

→ This suggests that there is necessity for long-range diffusion of Al atoms around Zr atoms during crystallization, which is difficult to achieve due to the presence of dense randomly packed clusters.

The presence of dense randomly packed atomic configurations in the glassy state of BMGs can also be inferred from the small changes in the relative densities of the fully glassy and the corresponding fully crystalline alloys (see Table 6.1). It is noted that the densities of the glassy alloys are lower than those in the crystallized state. The difference between the fully glassy and fully crystalline alloys is typically about 0.5%, but is occasionally as high as 1% (see, for example, Ref. [81]). Further, the density difference between the structurally relaxed and fully glassy states is about 0.11%–0.15%. Thus, the small density differences between the glassy and crystallized conditions suggest that the glassy alloys contain dense randomly packed clusters in them.

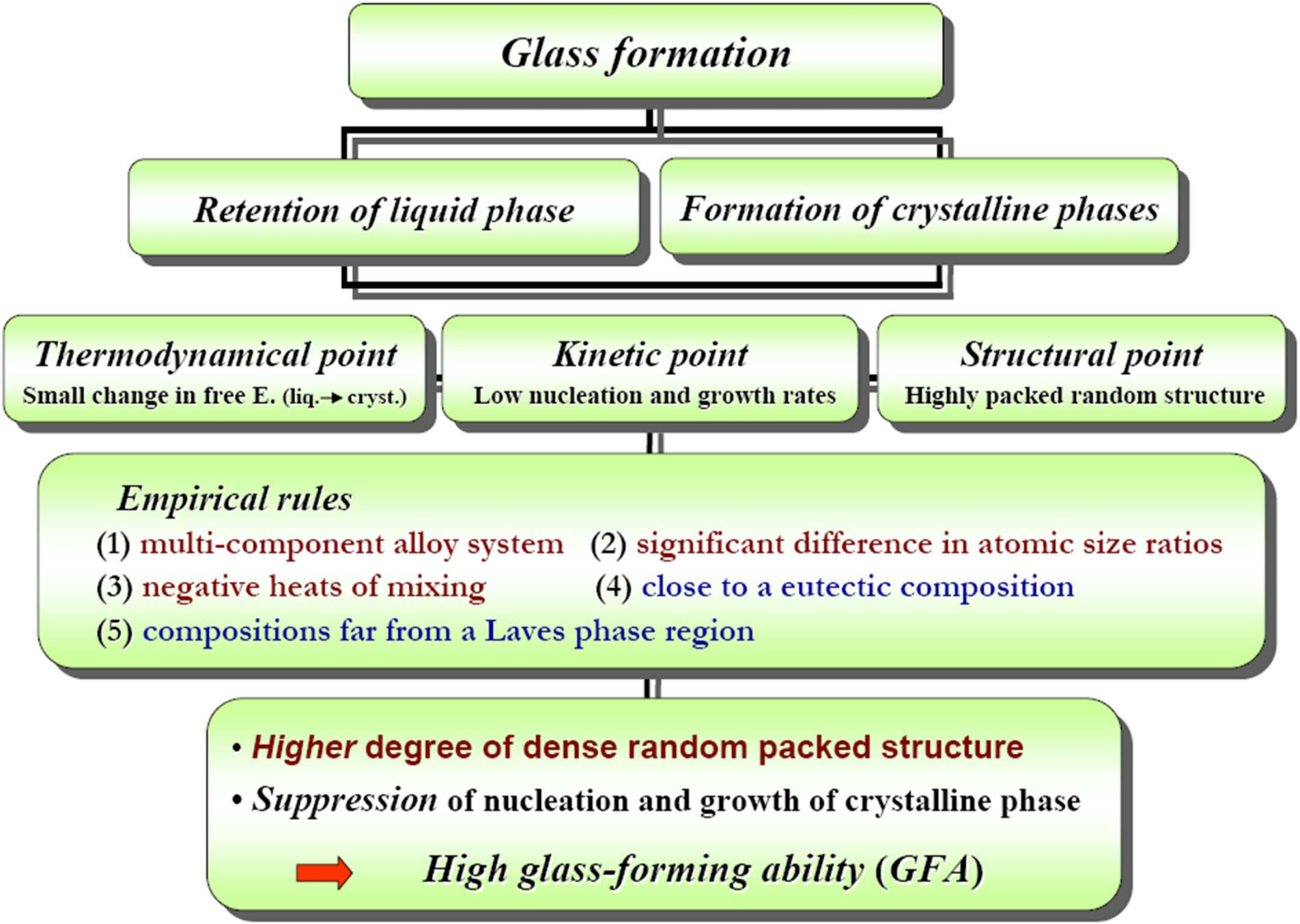
Glass formation
Retention of liquid phase
Formation of crystalline phases
Thermodynamical point
Small change in free E. (liq.→cryst.)
Kinetic point
Low nucleation and growth rates
Structural point
Highly packed random structure
Empirical rules
(1) multi-component alloy system
(2) significant difference in atomic size ratios
(3) negative heats of mixing
(4) close to a eutectic composition
(5) compositions far from a Laves phase region
• Higher degree of dense random packed structure
• Suppression of nucleation and growth of crystalline phase
High glass-forming ability (GFA)

Alloy design and new BMG development

Ca-Mg-Zn alloy system

- **Dense packed structure**

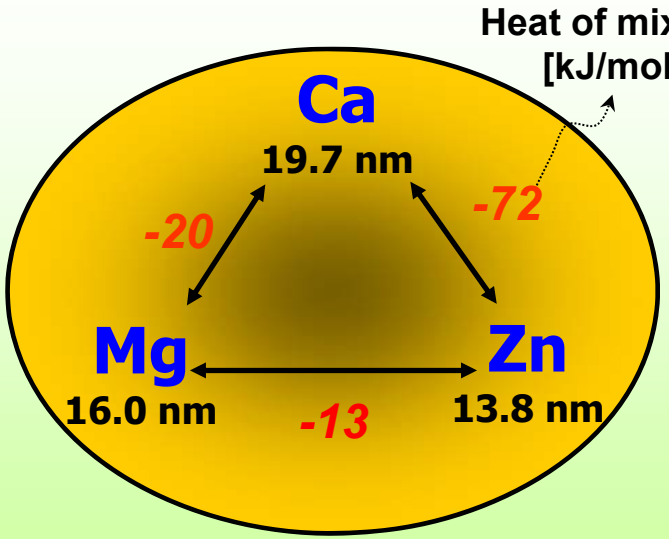

- Large difference in atomic size
- Large negative heat of mixing

- **Decrease of melting temp.**

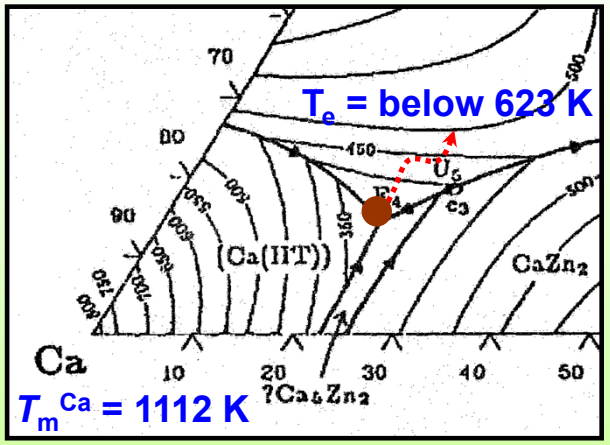

Deep eutectic condition

$$T_e / T_m^{Ca} = 0.560$$

Ca-Mg-Zn alloy system

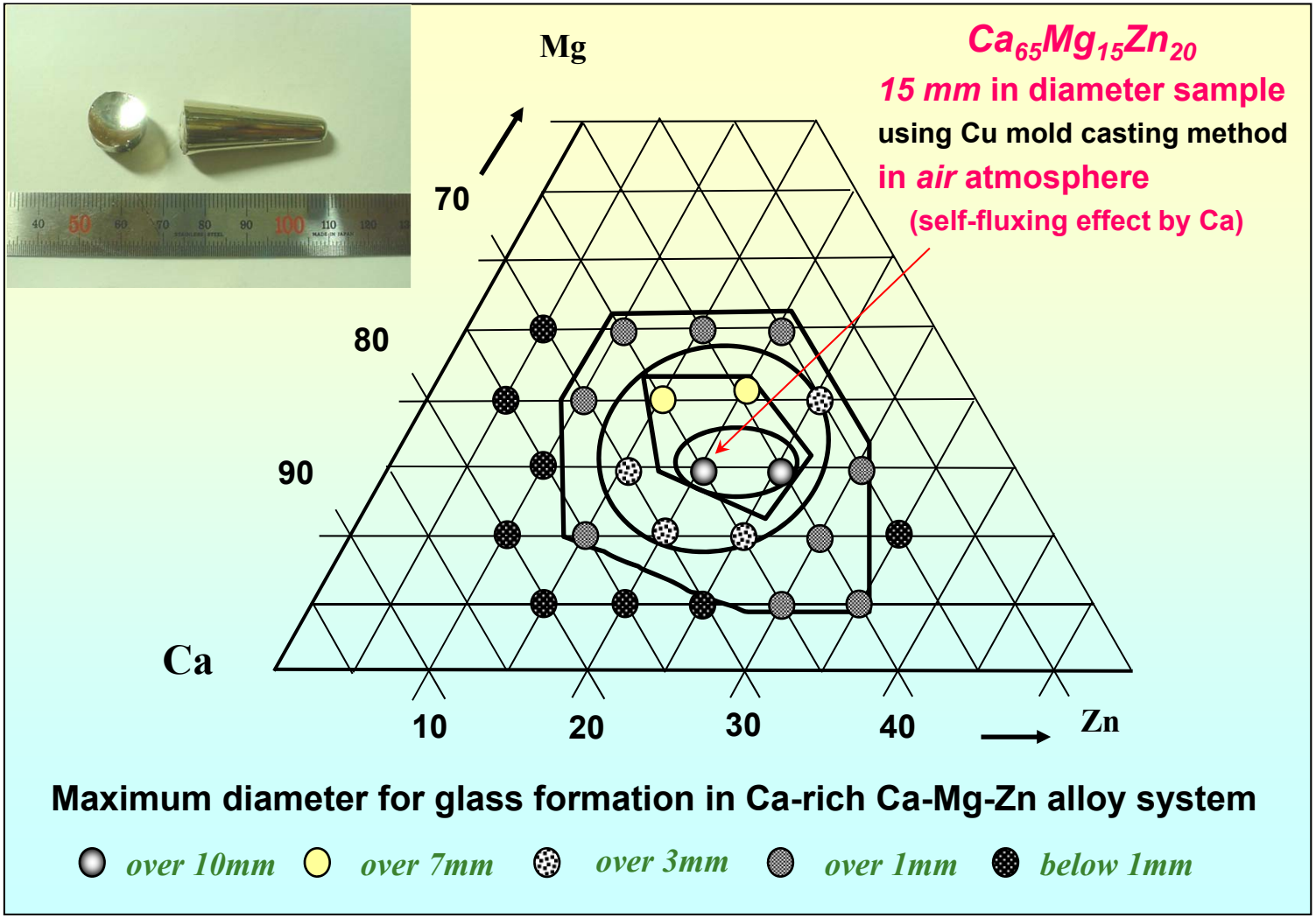

* J. Mater. Res. 19, 685 (2004)
* Mater. Sci. Forum 475-479, 3415 (2005)

3.8 Exceptions to the Above Criteria

3.8.1 Less Than Three Components in an Alloy System – Binary BMGs

One of the apparent exceptions to this empirical rule appears to be that BMGs have been produced in binary alloy systems such as Ca–Al [59], Cu–Hf [49], Cu–Zr [51], Ni–Nb [37], and Pd–Si [42].

Two important points:

1) The maximum diameter of the glassy rods obtained in these binary alloys is relatively small, i.e. a maximum of only about 2 mm.
2) The "glassy" rods of the binary BMG alloys often seem to contain some nanocrystalline phases. (?)

Even though glassy (BMG) alloys of 1 or 2 mm diameter are produced in binary alloy compositions., their GFA improves dramatically with the addition of a third component. This observation again proves that a minimum of three components is required to produce a BMG alloy with a reasonably large diameter.

Hattori et al. [90] had conducted very careful high-pressure experiments on elemental Zr and Ti using a newly developed in situ angle-dispersive XRD using a two-dimensional detector and x-ray transparent anvils. These authors noted that despite the disappearance of all the Bragg peaks in the one-dimensional energy-dispersive data, two-dimensional angle-dispersive data showed several intense Bragg spots even at the conditions where amorphization was reported in these two metals. This investigation clearly confirms that pure metals cannot be amorphized

3.8.2 Negative Heat of Mixing

Phase separation is generally expected to occur in alloy systems containing elements that exhibit a positive heat of mixing. This is indicated by the presence of a miscibility gap in the corresponding phase diagram. Therefore, if phase separation has occurred, one immediately concludes that the constituent elements have a positive heat of mixing

It has been suggested that it is theoretically possible to observe phase separation in alloy systems containing three or more elements, even though the heat of mixing is negative between any two elements in the alloy system. According to Meijering [94,95], a ternary alloy phase, consisting of components A, B, and C, can decompose into two phases with different compositions even when the enthalpy of mixing between any two components is negative. This is possible when the enthalpy of mixing, ΔH for one of the three possible binary alloy systems is significantly more negative than the others. For example, it is possible that in a ternary alloy system A–B–C, ΔH_{A-B} is much more negative than $\Delta H_{B-C} \approx \Delta H_{A-C}$. This argument suggests that a miscibility gap could be present in a ternary (or higher-order) BMG alloy system even when all the constituent elements have a negative enthalpy of mixing. In other words, phase separation is possible even in an alloy with a reasonably good GFA.

3.9 New Criteria: to develop better and more precise criteria to predict the GFA of alloy systems

All the new criteria that have been proposed in recent years to explain the high GFA of BMGs can be broadly grouped into the following categories:

1. *Transformation temperatures of glasses*. In this group, the GFA is explained on the basis of the characteristic transformation temperatures of the glasses such as T_g, T_x, and T_l, and the different combinations of these three parameters.

2. *Thermodynamic modeling*. Thermodynamic parameters such as heat of mixing are used in this group to predict the glass formation and evaluate GFA in a given alloy system.

3. *Structural and topological parameters*. In this group, consideration is given to the atomic sizes of the constituent elements, their electronegativity, electron-to-atom ratio, heat of mixing, etc. Majority of the work in this area has been due to Egami [107] and Miracle [108,109].

4. *Physical properties of alloys*. This group considers the physical properties of materials such as the viscosity of the melt, heat capacity, activation energies for glass formation and crystallization, bulk modulus, etc.

5. *Computational approaches*. These methods help in predicting the GFA of alloys from basic thermodynamic data [110,111], and without the necessity of actually conducting any experiments to synthesize the glass and determine the GFA.

3.10 Transformation Temperatures of Glasses

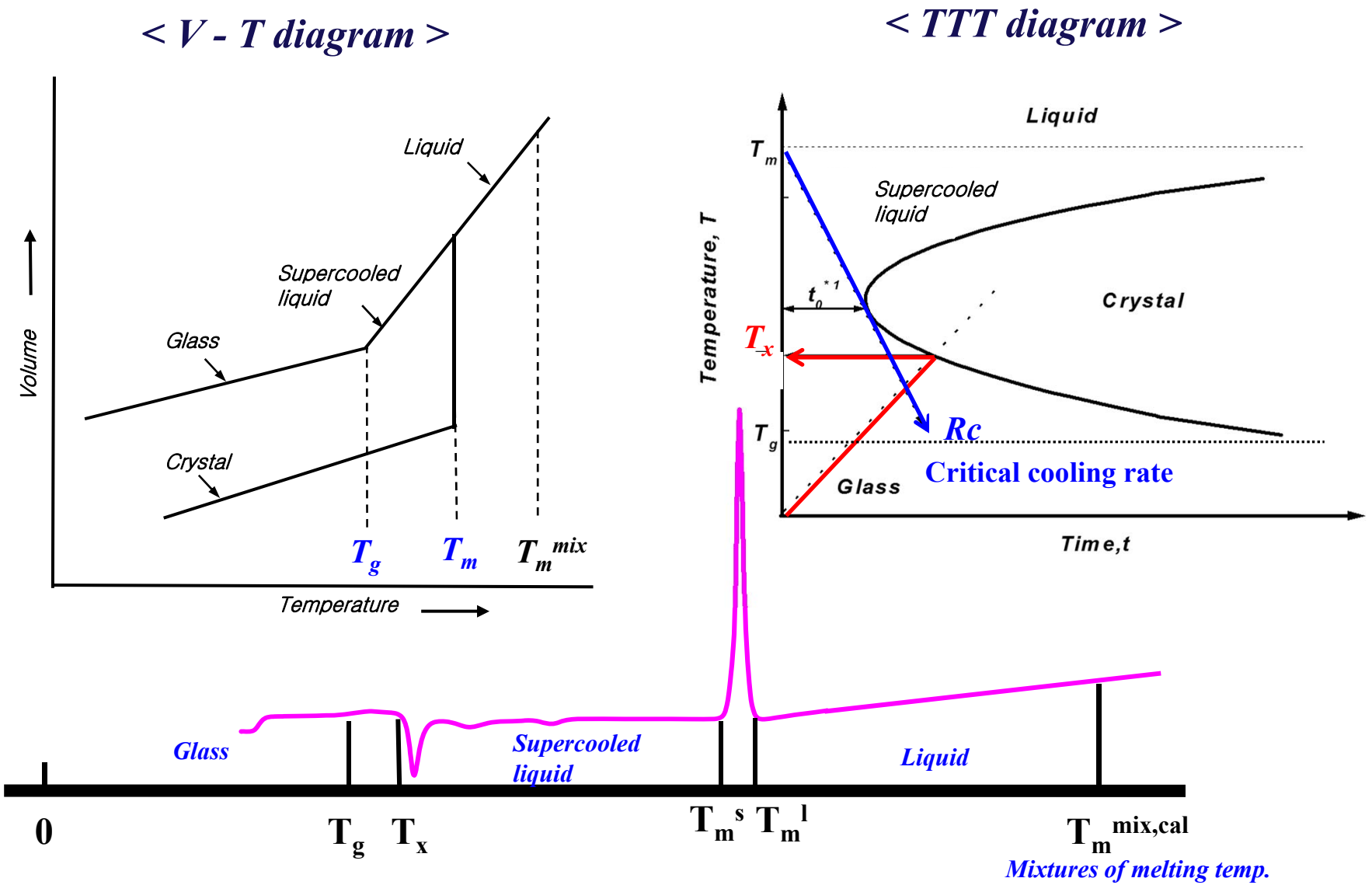

Representative GFA Parameters

Based on thermal analysis (T_g, T_x and T_l): thermodynamic and kinetic aspects

$T_{rg} = T_g/T_l$ — D. Turnbull et al., *Contemp. Phys.*, 10, 473 (1969)

$K = (T_x - T_g) / (T_l - T_x)$ — A. Hruby et al., *Czech.J.Phys.*, B22, 1187 (1972)

$\Delta T^* = (T_m^{mix} - T_l) / T_m^{mix}$ — I. W. Donald et al., *J. Non-Cryst. Solids*, 30, 77 (1978)

$\Delta T_x = T_x - T_g$ — A. Inoue et al., *J. Non-Cryst. Solids*, 156-158, 473 (1993)

$\gamma = T_x / (T_l + T_g)$ — Z.P. Lu and C. T. Liu, *Acta Materialia*, 50, 3501 (2002)

Based on thermodynamic and atomic configuration aspects

$\sigma = \Delta T^* \times P'$ — E. S. Park et al., *Appl. Phys. Lett.*, 86, 061907 (2005)

ΔT :* Relative decrease of melting temperature + *P'* : atomic size mismatch

: can be calculated simply using data on melting temp. and atomic size

GFA Parameters on the basis of thermodynamic or kinetic aspects :

1) ΔT_x parameter = $T_x - T_g$

- quantitative measure of glass stability toward crystallization upon reheating the glass above T_g: stability of glass state
- cannot be considered as a direct measure for GFA

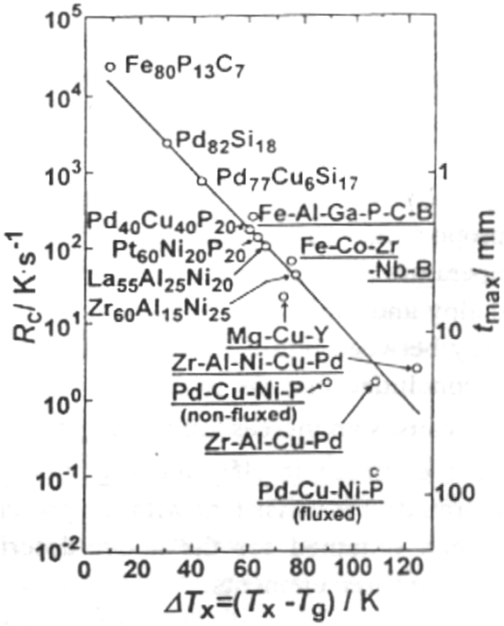

2) K parameter = $(T_x-T_g)/(T_l-T_x) = \Delta T_x/(T_l-T_x)$

- based on thermal stability of glass on subsequent reheating
- includes the effect of T_l , but similar tendency to ΔT_x

3) ΔT^* parameter = $(T_m^{mix} - T_l)/ T_m^{mix}$

- $$T_m^{mix} = \sum_i^n n_i \cdot T_m^i$$

(where n_i and T_m^i are the mole fraction and melting point, respectively, of the i th component of an n-component alloy.)

- evaluation of the stability of the liquid at equilibrium state
- alloy system with deep eutectic condition ~ good GFA
- for multi-component BMG systems: insufficient correlation with GFA

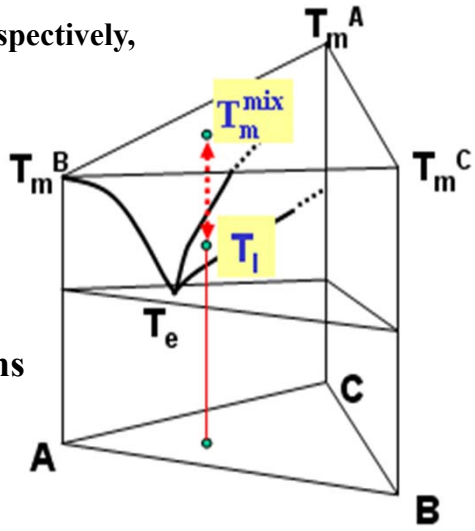

➡ T_m^{mix} represents the fractional departure of T_m with variation of compositions and systems from the simple rule of mixtures melting temperature

Time Temperature Transformation diagram:

1) $\Delta T_x = T_x - T_g$

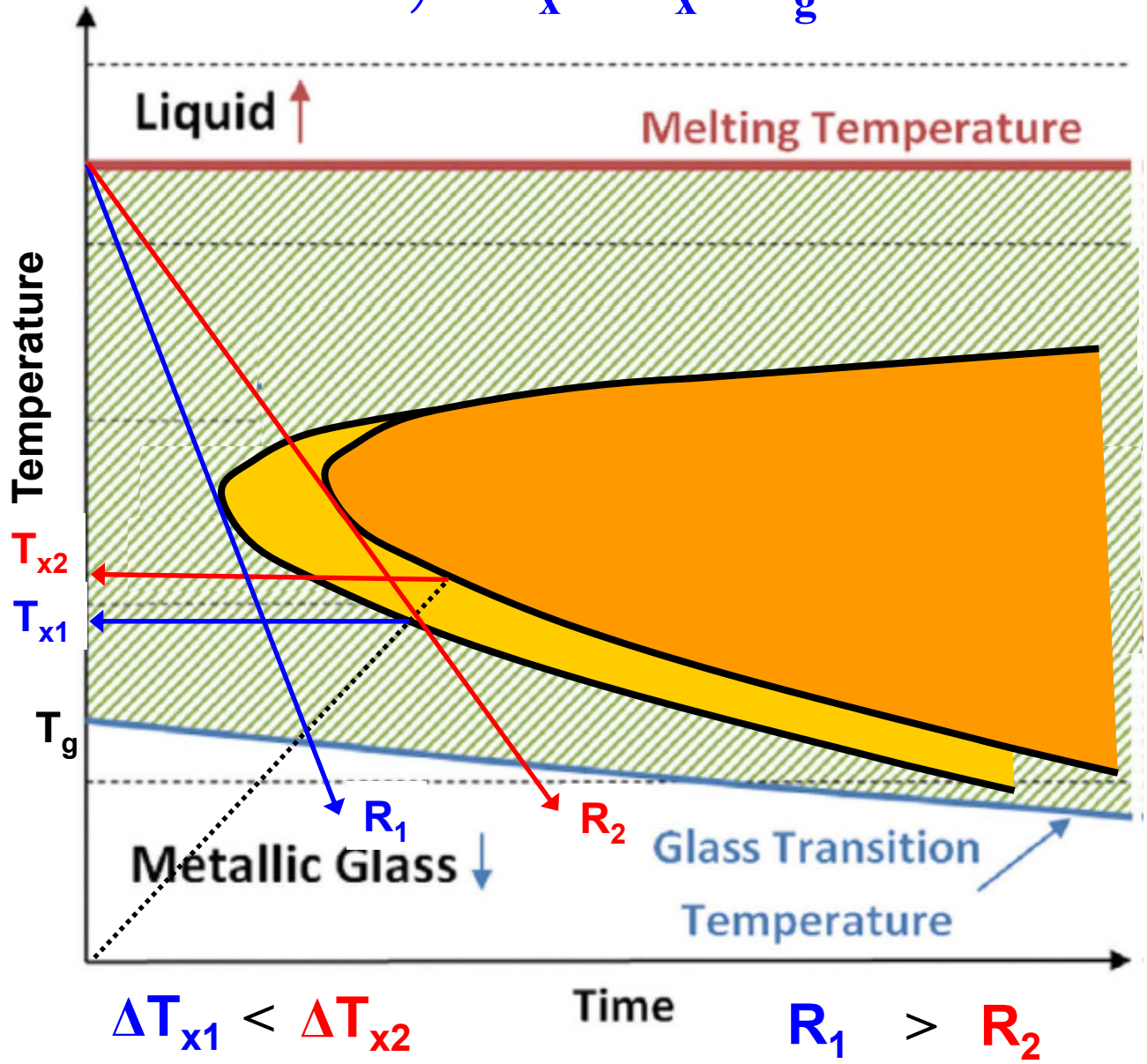

From the above discussion, it is clear that the description of the GFA of alloys using the ΔT_x parameter as a criterion has not been found universally applicable in all situations and for all alloy systems. Some exceptions have been certainly noted. But, it should, however, be emphasized in this context that this was one of the most successful parameters in the early years of research on BMGs.

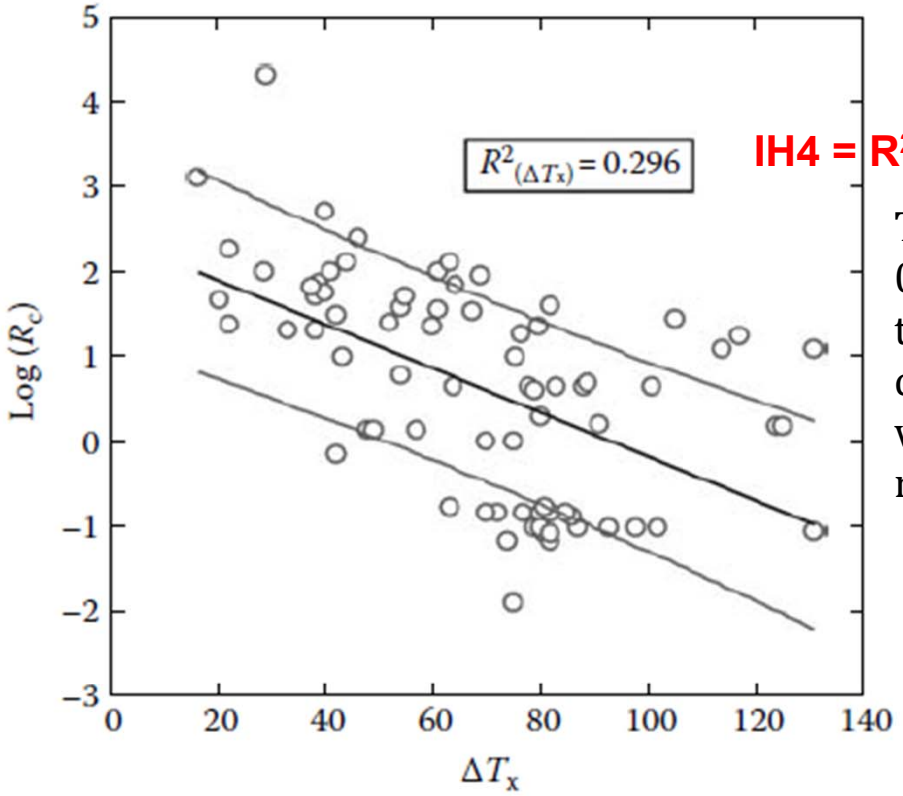

IH4 = R^2 : regression coefficient

The R^2 vale can range from 0 to 1 and is an indicator of the reliability of the correlation. The higher R^2 value, the more reliable the regression is.

FIGURE 3.5
Variation of the critical cooling rate, R_c with the width of the supercooled liquid region, ΔT_x for a number of multicomponent bulk metallic glasses. Data for some of the binary and ternary metallic glasses reported earlier are also included for comparison.

GFA Parameters on the basis of thermodynamic or kinetic aspects :

1) ΔT_x parameter = $T_x - T_g$

- quantitative measure of glass stability toward crystallization upon reheating the glass above T_g: stability of glass state
- cannot be considered as a direct measure for GFA

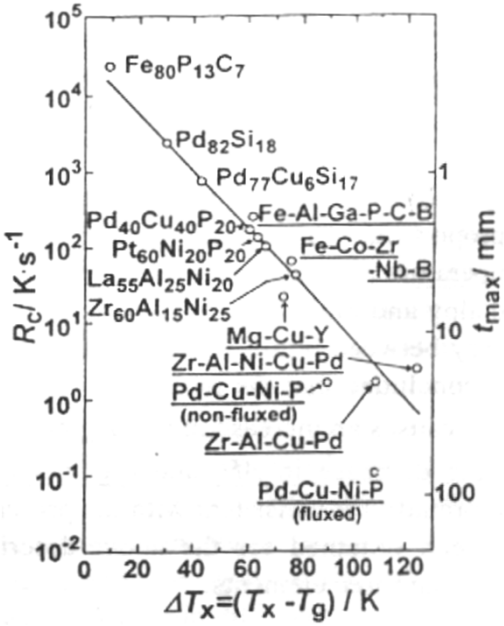

2) K parameter = $(T_x-T_g)/(T_l-T_x) = \Delta T_x/(T_l-T_x)$

- based on thermal stability of glass on subsequent reheating
- includes the effect of T_l , but similar tendency to ΔT_x

3) ΔT^* parameter = $(T_m^{mix} - T_l)/ T_m^{mix}$

- $$T_m^{mix} = \sum_i^n n_i \cdot T_m^i$$

(where n_i and T_m^i are the mole fraction and melting point, respectively, of the i th component of an n-component alloy.)

- evaluation of the stability of the liquid at equilibrium state
- alloy system with deep eutectic condition ~ good GFA
- for multi-component BMG systems: insufficient correlation with GFA

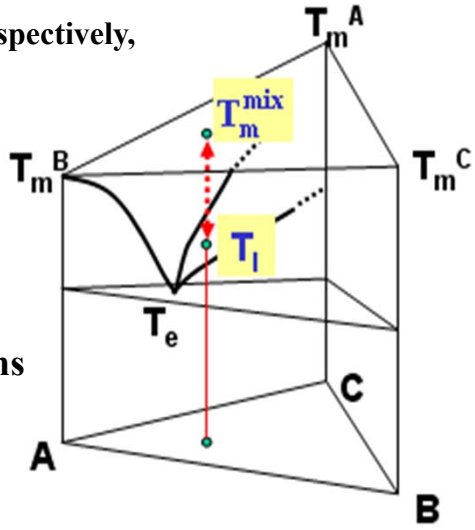

➡ T_m^{mix} represents the fractional departure of T_m with variation of compositions and systems from the simple rule of mixtures melting temperature

Time Temperature Transformation diagram:

2) $K=(T_x-T_g)/(T_l-T_x)=\Delta T_x/(T_l-T_x)$

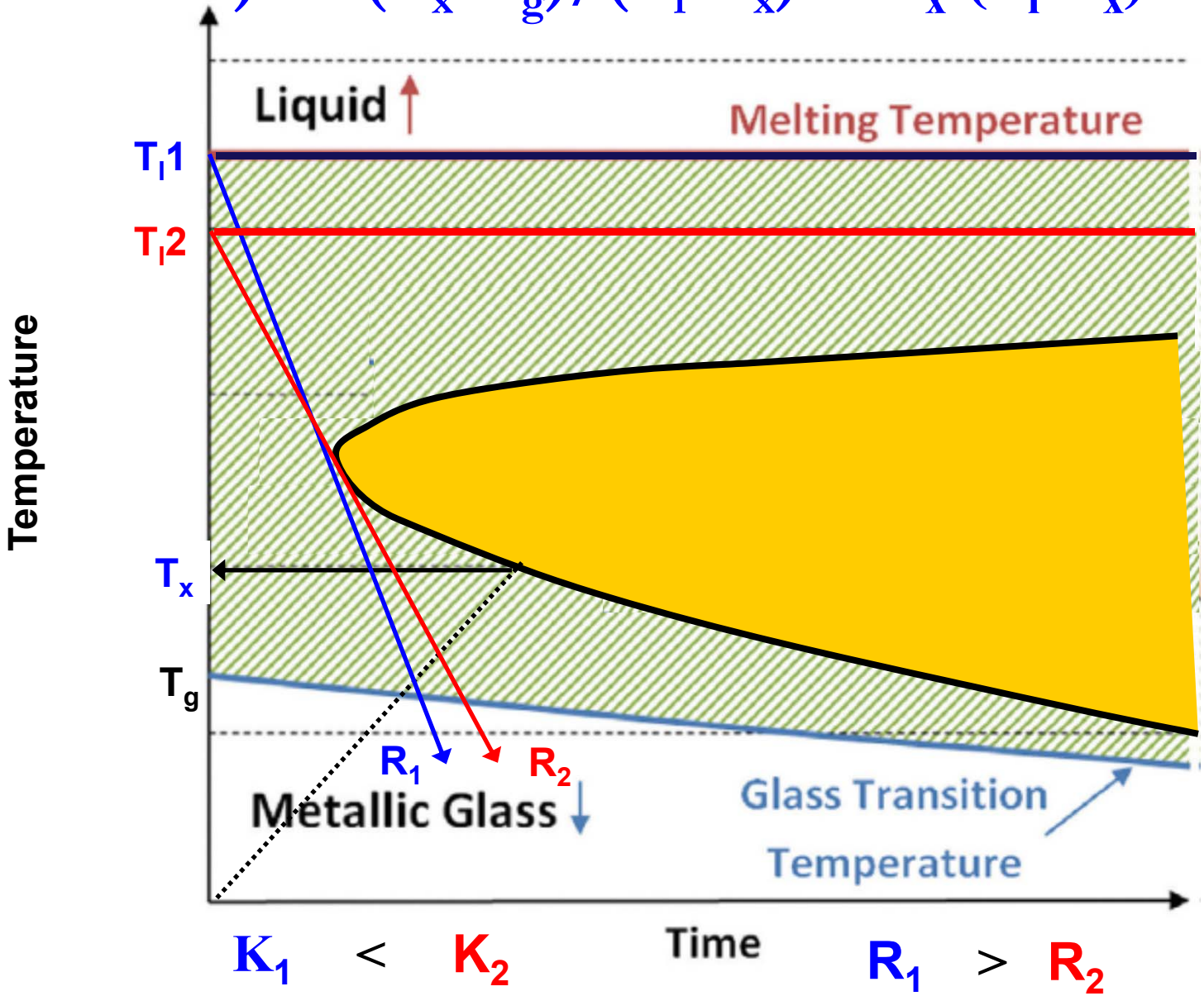

GFA Parameters on the basis of thermodynamic or kinetic aspects :

1) ΔT_x parameter = $T_x - T_g$

- quantitative measure of glass stability toward crystallization upon reheating the glass above T_g: stability of glass state
- cannot be considered as a direct measure for GFA

2) K parameter = $(T_x-T_g)/(T_l-T_x) = \Delta T_x/(T_l-T_x)$

- based on thermal stability of glass on subsequent reheating
- includes the effect of T_l , but similar tendency to ΔT_x

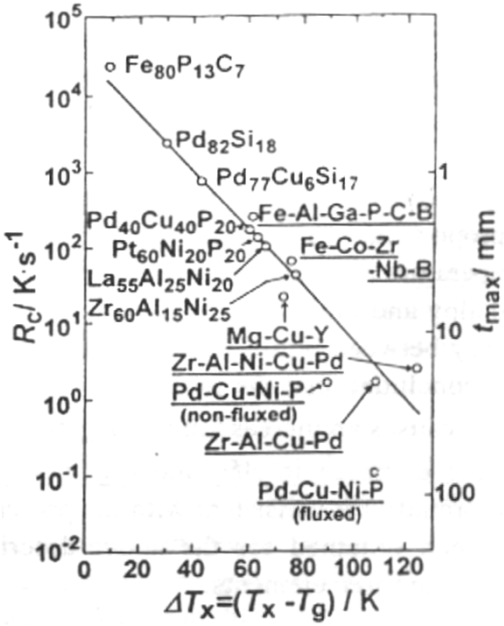

3) ΔT^* parameter = $(T_m^{mix} - T_l)/ T_m^{mix}$

- $$T_m^{mix} = \sum_i^n n_i \cdot T_m^i$$

(where n_i and T_m^i are the mole fraction and melting point, respectively, of the i th component of an n-component alloy.)

- evaluation of the stability of the liquid at equilibrium state
- alloy system with deep eutectic condition ~ good GFA
- for multi-component BMG systems: insufficient correlation with GFA

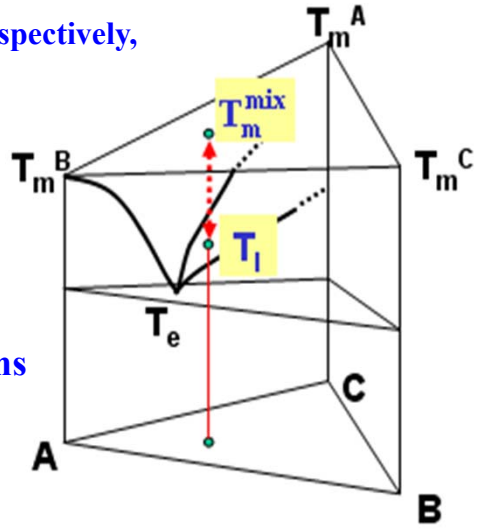

→ T_m^{mix} represents the fractional departure of T_m with variation of compositions and systems from the simple rule of mixtures melting temperature

Relative decrease of melting temperature

$$\Delta T^* = \frac{T_m^{mix} - T_l}{T_m^{mix}}$$

: ratio of Temperature difference between liquidus temp. T_l and imaginary melting temp. T_m^{mix} to T_m^{mix}

(where, $T_m^{mix} = \sum x_i T_m^i$, x_i = molefraction, T_m^i = melting point)

by I.W. Donald et al. (*J. Non-Cryst. Solids*, 30, 77 (1978))

➡ $\Delta T^* \geq 0.2$ in most of glass forming alloys

Ca-Mg-Zn alloy system

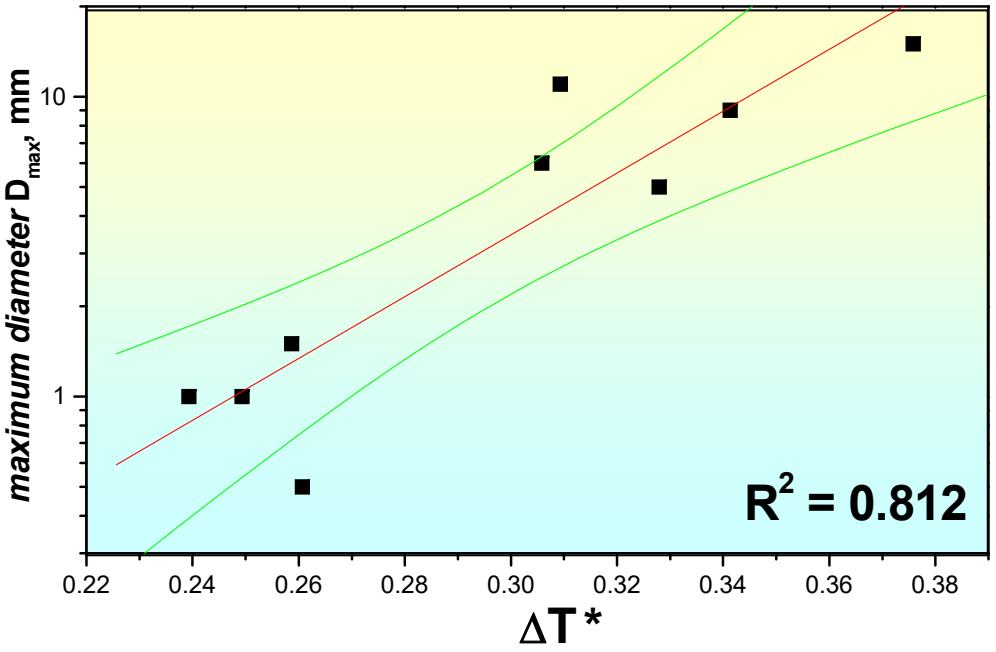

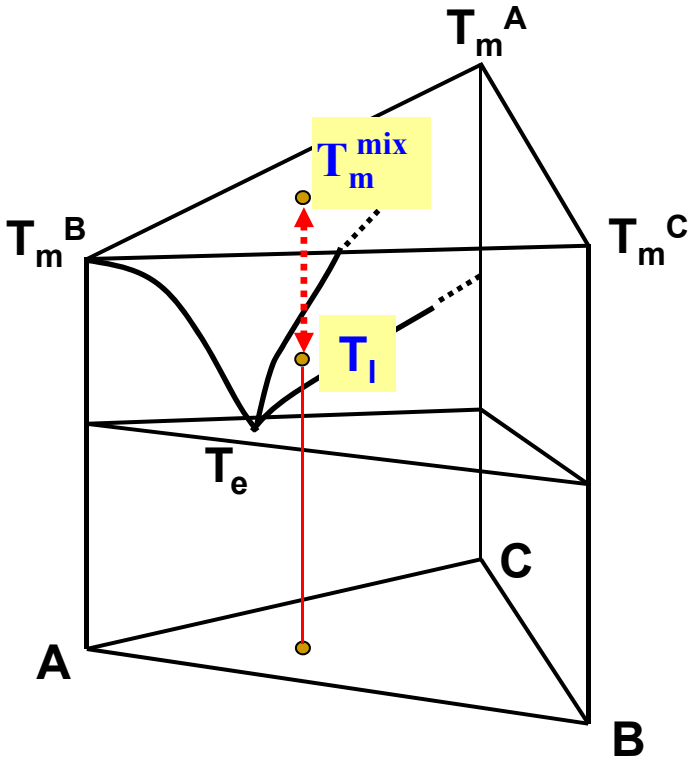

GFA Parameters on the basis of thermodynamic or kinetic aspects :

4) T_{rg} parameter = T_g/T_l

- kinetic approach to avoid crystallization before glass formation
- Viscosity at T_g being constant, the higher the ratio T_g/T_l, the higher will be the viscosity at the nose of the CCT curves, and hence the smaller R_c
- T_l ↓and T_g ↑ ► lower nucleation and growth rate ► GFA ↑

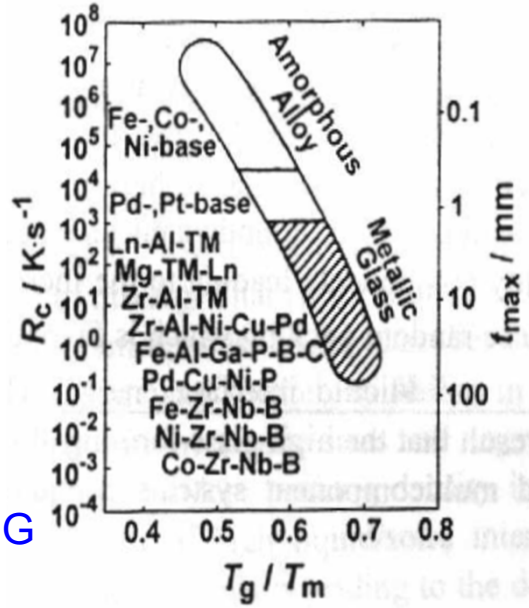

- ▪ significant difference between T_l and T_g in multi-component BMG
- ▪ insufficient information on temperature-viscosity relationship
- ► insufficient correlation with GFA

5) γ parameter = T_x / (T_l + T_g)

- thermodynamic and kinetic view points - relatively reliable parameter
- stability of equilibrium and metastable liquids: T_l and T_g
- resistance to crystallization: T_x

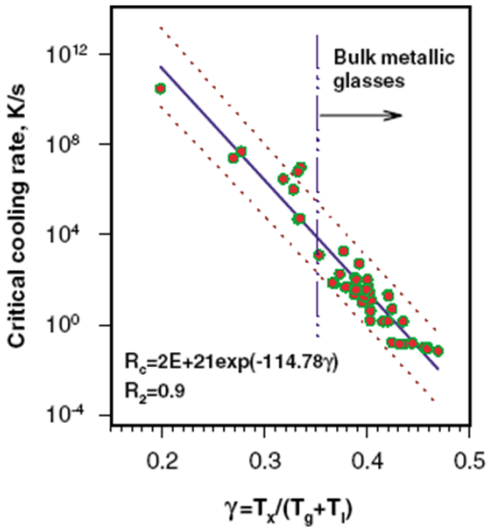

T_{rg} parameter $= T_g/T_l \sim \eta$: the higher T_{rg}, the higher η, the lower R_c

: ability to avoid crystallization during cooling

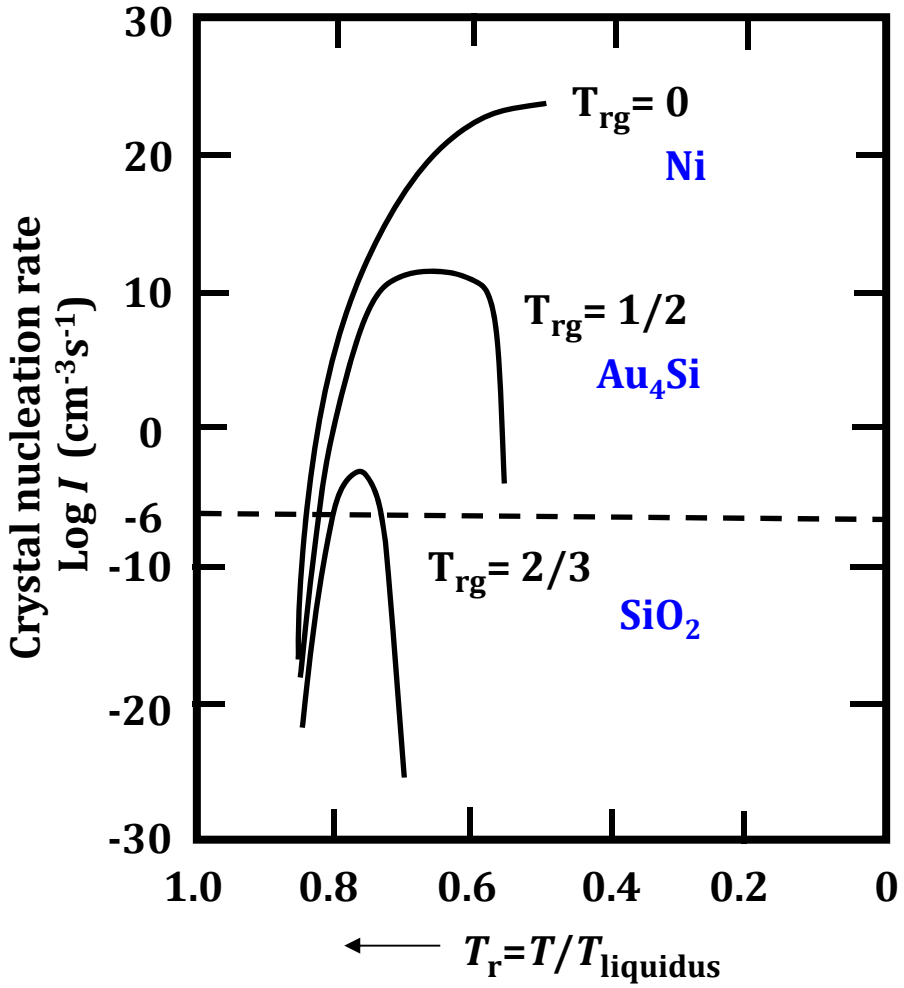

$T_{rgNi} < T_{rgAu4Si} < T_{rgSiO2}$

$R_{Ni} > R_{Au4Si} > R_{SiO2}$

Turnbull, 1959 ff.

Time Temperature Transformation diagram:

$T_{rg}=T_g/T_l$

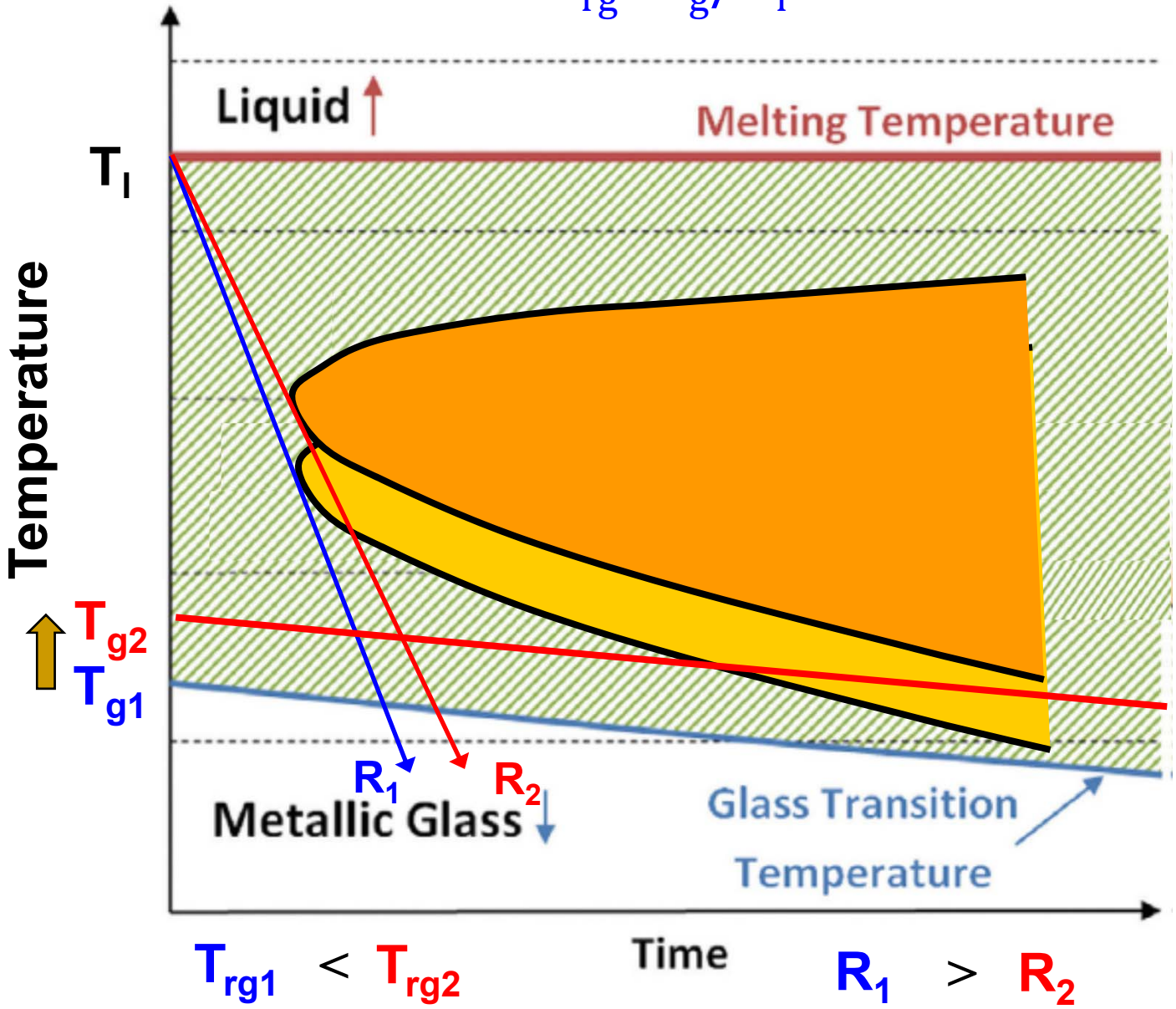

Time Temperature Transformation diagram:

$$T_{rg} = T_g / T_l$$

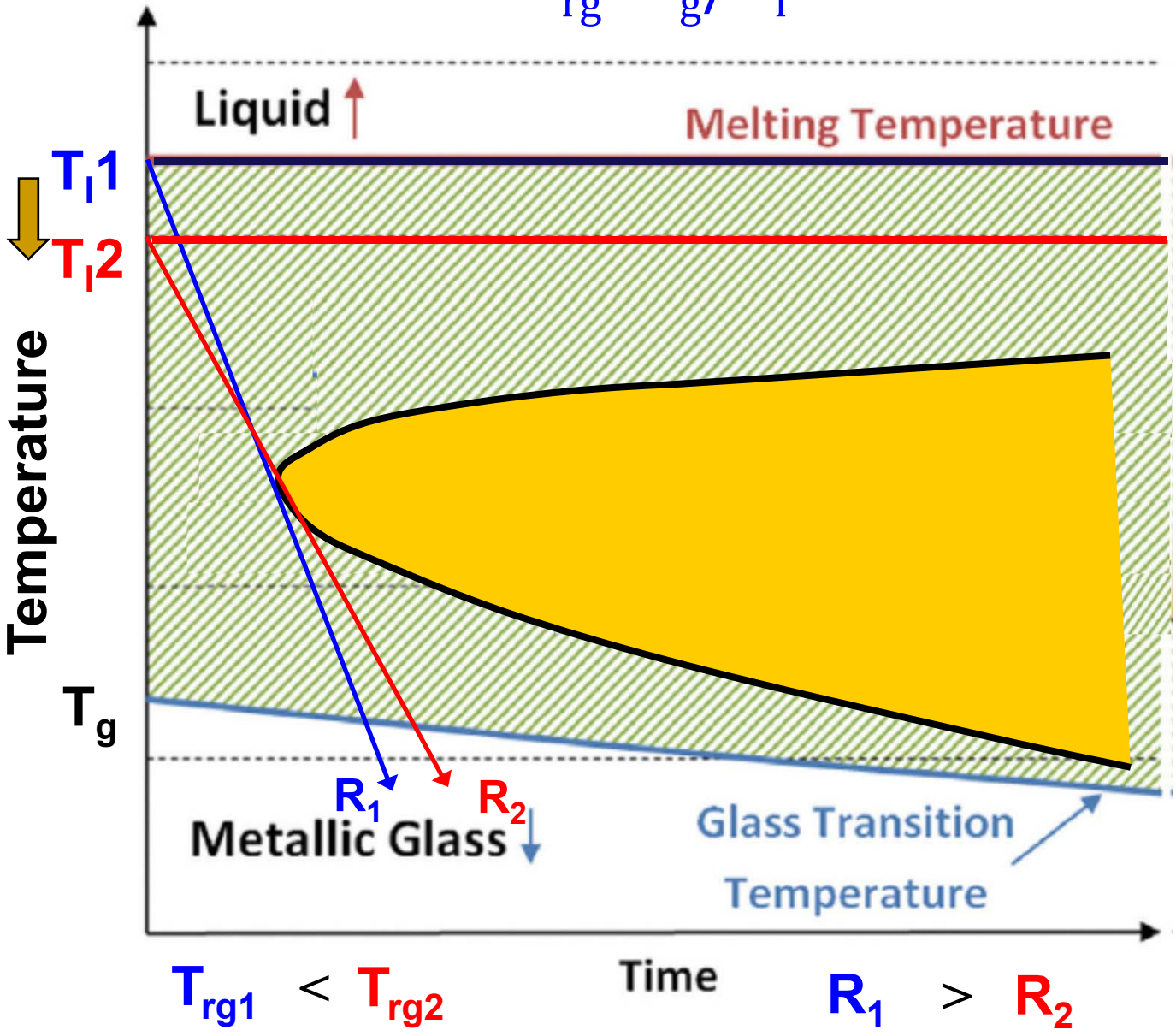

GFA Parameters on the basis of thermodynamic or kinetic aspects :

4) T_{rg} parameter = T_g/T_l

- kinetic approach to avoid crystallization before glass formation
- Viscosity at T_g being constant, the higher the ratio T_g/T_l, the higher will be the viscosity at the nose of the CCT curves, and hence the smaller R_c
- T_l ↓and T_g ↑ ► lower nucleation and growth rate ► GFA ↑

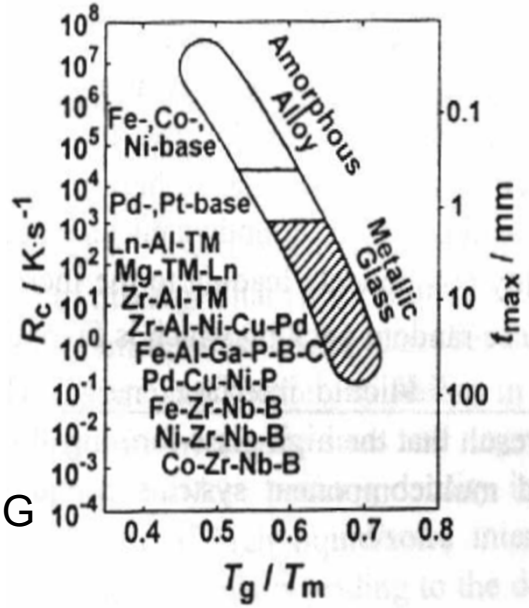

- ▪ significant difference between T_l and T_g in multi-component BMG
- ▪ insufficient information on temperature-viscosity relationship
- ► insufficient correlation with GFA

5) γ parameter = T_x / (T_l + T_g)

- thermodynamic and kinetic view points - **relatively reliable parameter**
- stability of equilibrium and metastable liquids: T_l and T_g
- resistance to crystallization: T_x

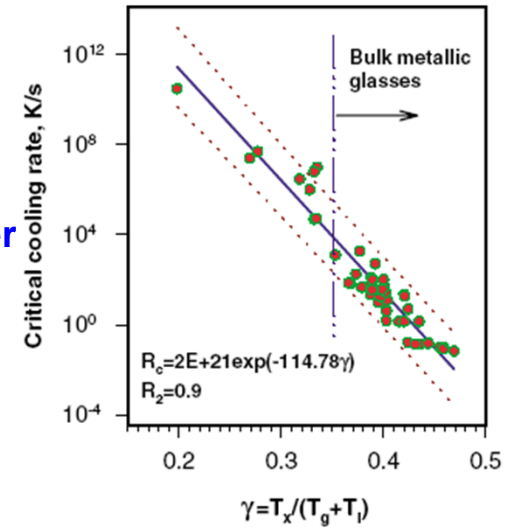

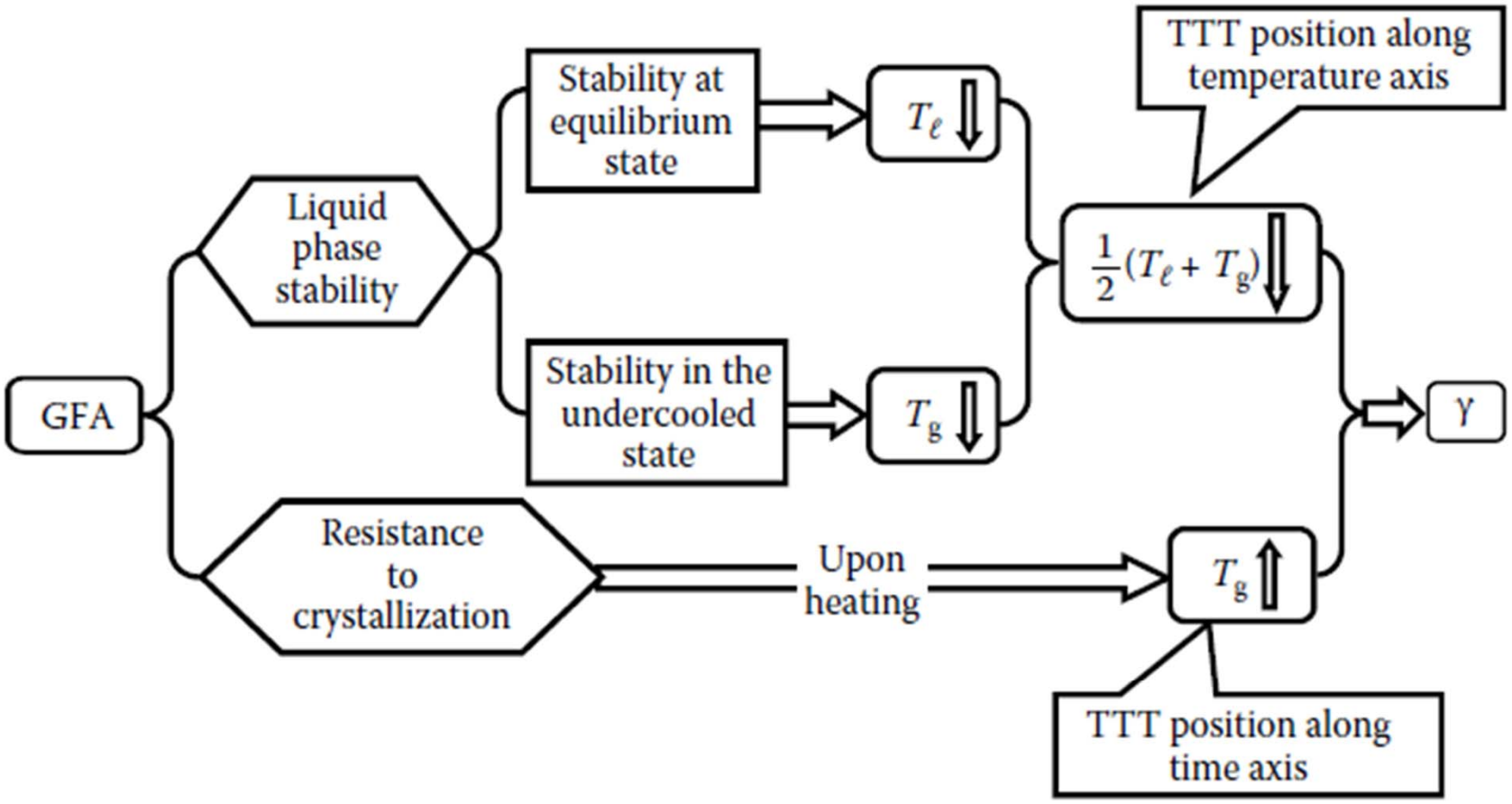

FIGURE 3.8
Schematic to illustrate the different factors involved in deriving the γ parameter to explain the GFA of alloys. (Reprinted from Lu, Z.P. and Liu, C.T., *Intermetallics*, 12, 1035, 2004. With permission.)

$$\gamma \propto T_x\left[\frac{1}{2(T_g + T_l)}\right] \propto \frac{T_x}{T_g + T_l}$$

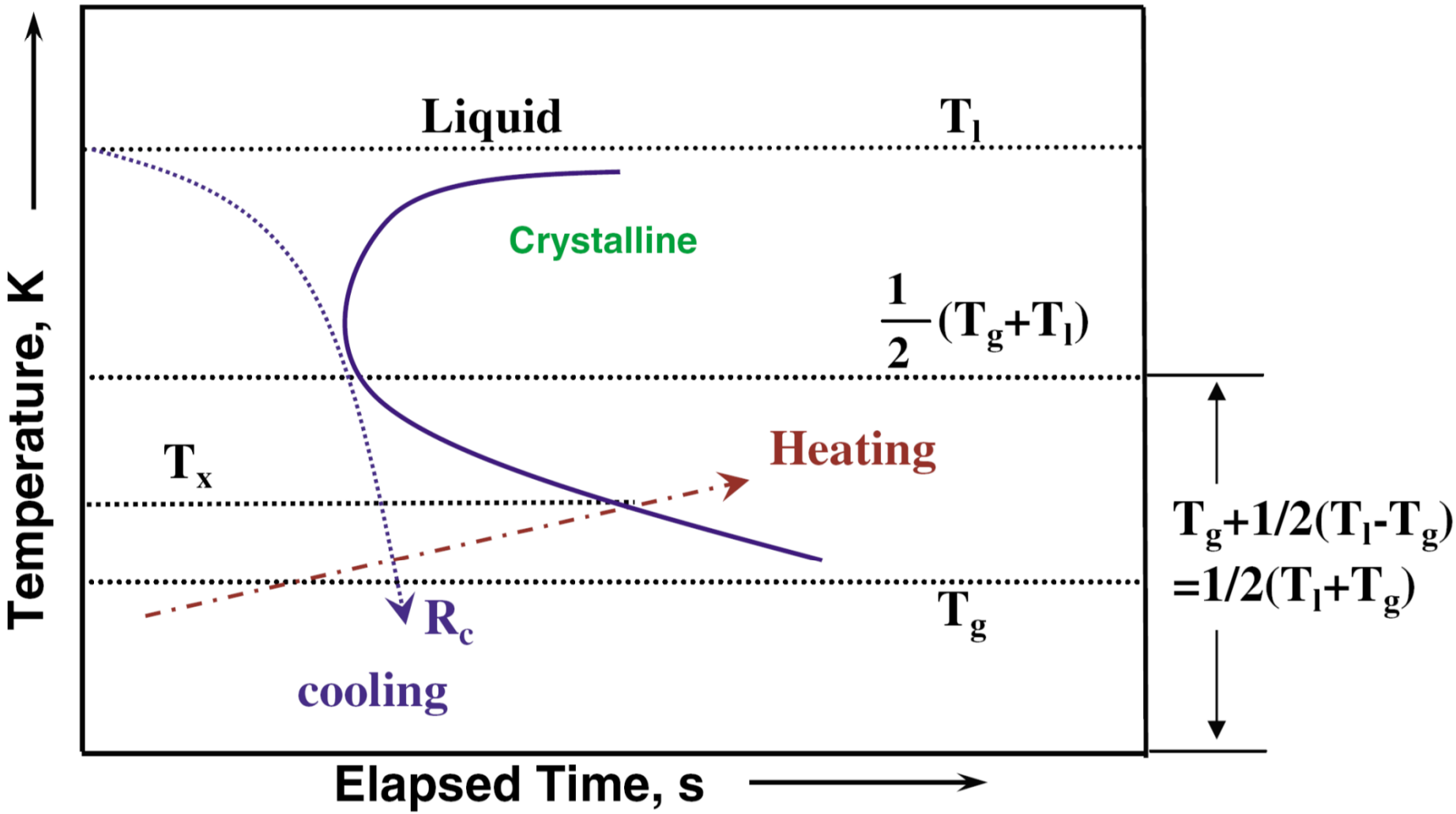

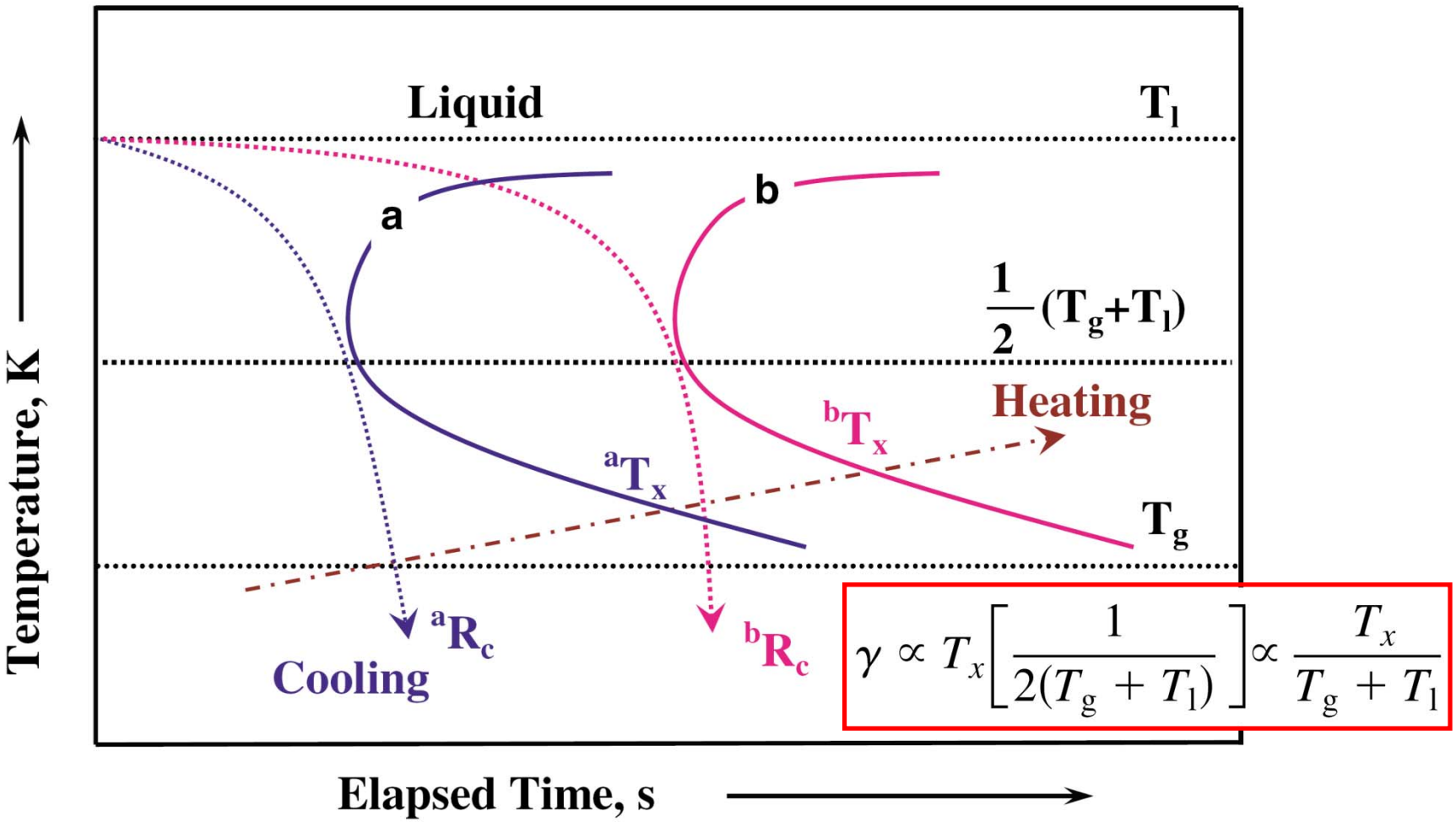

FIG. 2 (color online). Schematic TTT curves showing the effect of T_x measured upon continuous heating for different liquids with similar T_l and T_g; liquid b with higher onset crystallization temperature ^bT_x ($^aT_x < {}^bT_x$) shows a lower critical cooling rate ^bR_c ($^bR_c < {}^aR_c$).

$$\log_{10} R_c = (21.71 \pm 1.97) - (50.90 \pm 0.71)\gamma \qquad \log_{10} t_{max} = (-6.55 \pm 1.07) + (18.11 \pm 0.70)\gamma$$

$$R_c = R_0 \exp\left[\left(-\frac{\ln R_0}{\gamma_0}\right)\gamma\right] \qquad t_{max} = t_0 \exp\left[\left(-\frac{\ln t_0}{\gamma_1}\right)\gamma\right]$$

$$R_c = 5.1 \times 10^{21} \exp(-117.2\gamma) \qquad t_{max} = 2.80 \times 10^{-7} \exp(41.7\gamma)$$

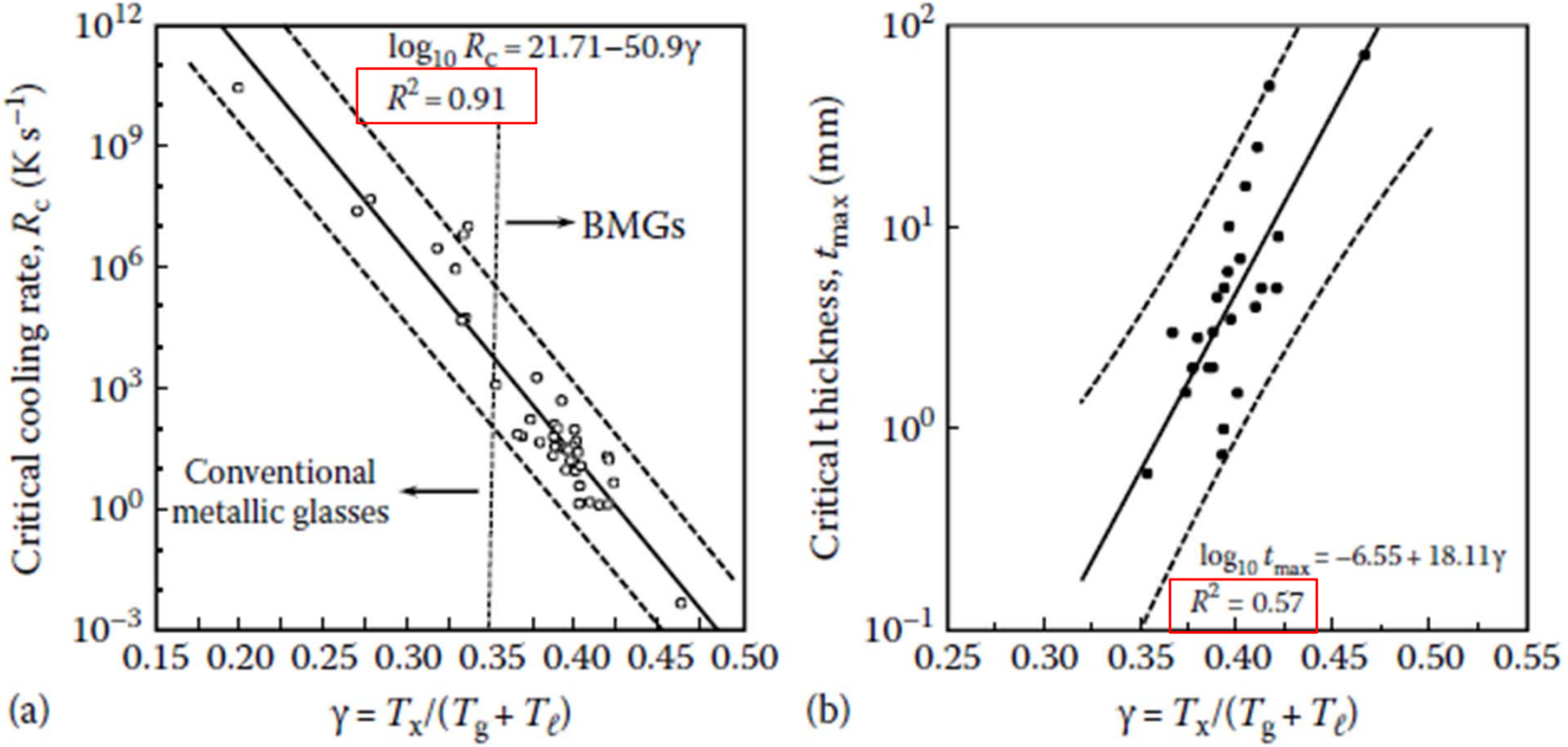

Wide scatter for the t_{max} correlation

FIGURE 3.9

(a) Correlation between the critical cooling rate (R_c) and the γ parameter for BMGs. (b) Correlation between the maximum section thickness (t_{max}) and the γ parameter for BMGs. (Reprinted from Lu, Z.P. and Liu, C.T., *Acta Mater.*, 50, 3501, 2002. With permission.)

GFA Parameters *on the basis of thermodynamic or kinetic aspects*

GFA parameters	Expression	Year established	
T_{rg}	T_g / T_l	1969	D.Turnbull,Contemp.Phys.10(1969) 473
K	$(T_x-T_g) / (T_l-T_x)$	1972	A.Hruby, Czech. J.Phys. B 22 (1972) 1187
ΔT^*	$(T_m^{mix}-T_l) / T_m^{mix}$	1978	I.W.Donald, J.Non-Cryst.Solids 30 (1978) 77
ΔT_x	$T_x - T_g$	1993	A.Inoue, J.Non-Cryst.Solids 156-158(1993)473
γ	$T_x / (T_l+T_g)$	2002	Z.P.Lu, C.T.Liu, Acta Mater. 50 (2002) 3501
δ	$T_x / (T_l-T_g)$	2005	Q.J.Chen,Chiness Phys.Lett.22 (2005) 1736
α	T_x / T_l	2005	K.Mondal, J.Non-Cryst.Solids 351(2005) 1366
β	$T_x / T_g + T_g / T_l$	2005	K.Mondal, J.Non-Cryst.Solids 351(2005) 1366
φ	$(T_g / T_l)(T_x-T_g / T_g)^a$	2007	G.J.Fan,J.Non-Cryst. Solids 353 (2007) 102
γ_m	$(2T_x - T_g) / T_l$	2007	X.H.Du,J.Appl.phys.101 (2007) 086108
β	$(T_g / T_l - T_g)(T_g / T_l - T_g)$	2008	Z.Z.Yuan, J. Alloys Compd.459 (2008)
ξ	$\Delta T_x / T_x + T_g / T_l$	2008	X.H.Du,Chinese Phys.B 17(2008) 249

No universal model **to predict and evaluate what families of alloy compositions are likely to form BMGs**

Combination of categories

that are viewed as decisive in the formation of amorphous alloys

New criterion

for predicting and evaluating Glass Forming Ability

- **useful guideline for BMG alloy system design**

- save time and experimental cost

→ **new alloy system with enhanced GFA**

Approach 1. combine thermodynamic and structural points

$$\sigma = \Delta T^{*} \times \quad P'$$

ΔT^{*} : **Relative decrease of melting temp.** $\boldsymbol{P'}$: **Effective atomic mismatch per solute atom**

$$\Delta T^{*} = \frac{T_m^{mix} - T_l}{T_m^{mix}}$$

$$P' = \frac{C_B}{C_B + C_C}\left|\frac{v_B - v_A}{v_A}\right| + \frac{C_C}{C_B + C_C}\left|\frac{v_C - v_A}{v_A}\right|$$

(where, $T_m^{mix} = \sum x_i T_m^i$, x_i = molefraction, T_m^i = melting point)

(where, C_i(i=A,B,C) = solute content, v_i = atomic volume)

Approach 2. combine thermodynamic and kinetic points

$$\varepsilon = \frac{\Delta T_m + \Delta T_x + T_x}{T_m^{mix}}$$

$\Delta Tm + \Delta Tx$: ***Liquid phase stability*** + $\boldsymbol{Tx}$: ***Resistance to cristallization***

(where, ΔTm = Tmmix – Tl , ΔTx = Tx – Tg)

(where, Tx = crystallization onset temperature)

Ca-Mg-Zn alloy system

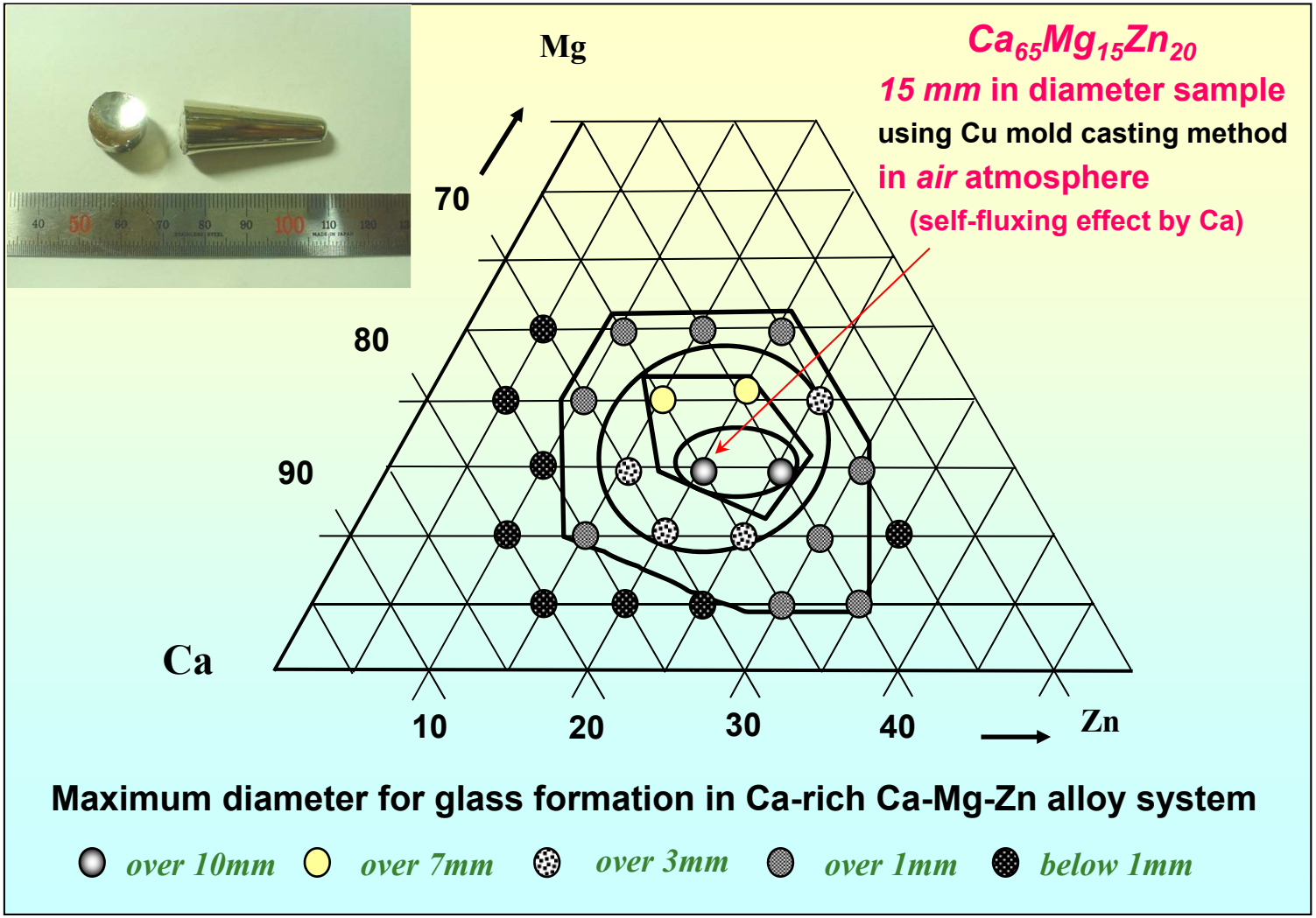

* J. Mater. Res. 19, 685 (2004)
* Mater. Sci. Forum 475-479, 3415 (2005)

Thermodynamic aspect for glass formation

Relative decrease of melting temperature

: ratio of Temperature difference between liquidus temp. T_l and imaginary melting temp. T_m^{mix} to T_m^{mix}

$$\Delta T^* = \frac{T_m^{mix} - T_l}{T_m^{mix}}$$

(where, $T_m^{mix} = \sum x_i T_m^i$, x_i = molefraction, T_m^i = melting point)

by I.W. Donald et al. (*J. Non-Cryst. Solids*, 30, 77 (1978))

➡ $\Delta T^* \geq 0.2$ in most of glass forming alloys

Ca-Mg-Zn alloy system

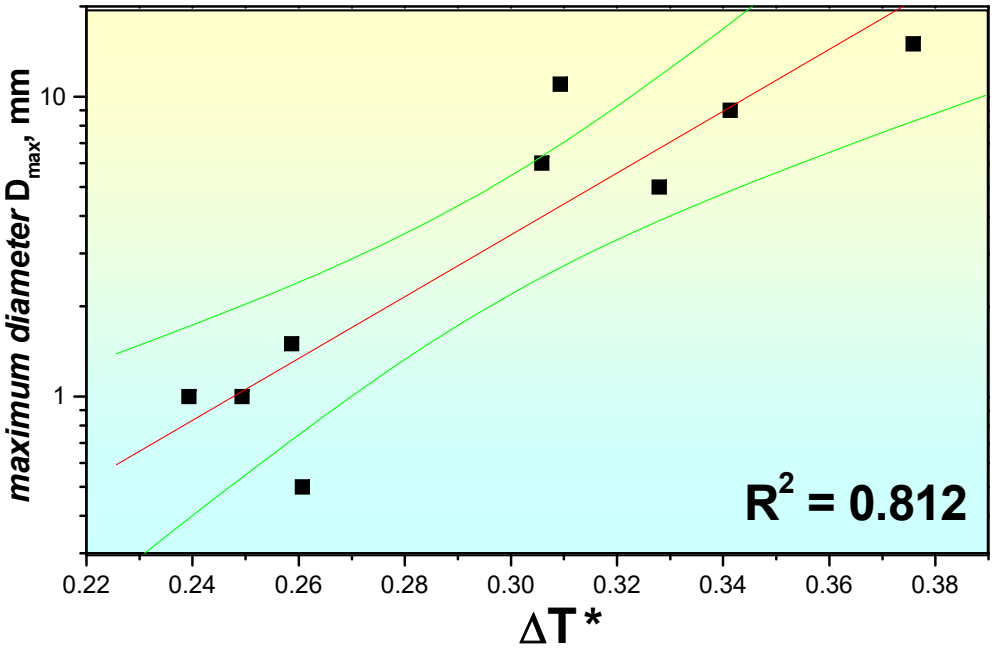

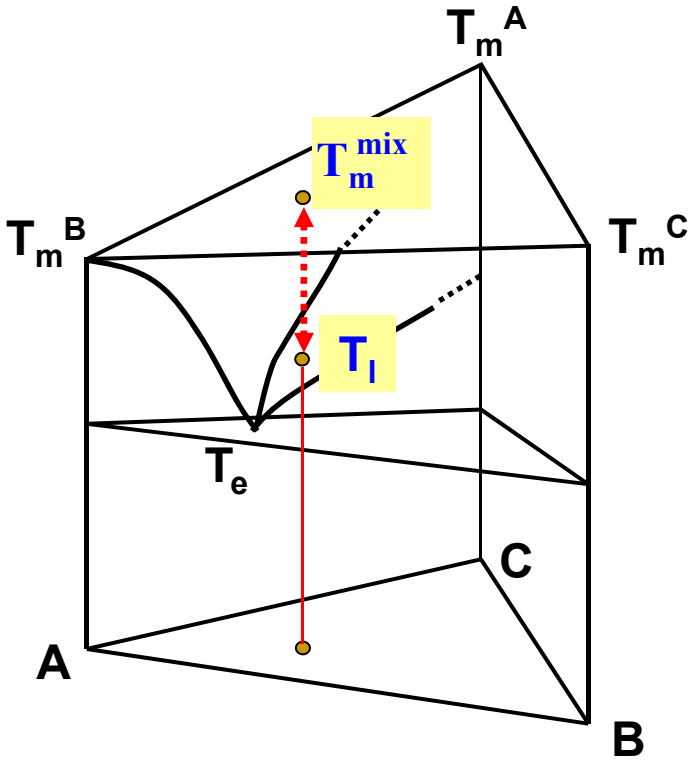

Structural aspect for glass formation

- **Effect of atomic size difference can be represented as follows;**

$$P = C_B \left| \frac{v_B - v_A}{v_A} \right| + C_C \left| \frac{v_C - v_A}{v_A} \right|$$

$$P' = \frac{C_B}{C_B + C_C} \left| \frac{v_B - v_A}{v_A} \right| + \frac{C_C}{C_B + C_C} \left| \frac{v_C - v_A}{v_A} \right|$$

Where, C_i(i=A,B,C) = solute, v_i = content atomic volume ; effective atomic mismatch of solute atom

by dividing by the total amount of solute contents

* Metall.& Mater. Trans. A 32, 200 (2001)

Ca-Mg-Zn alloy system

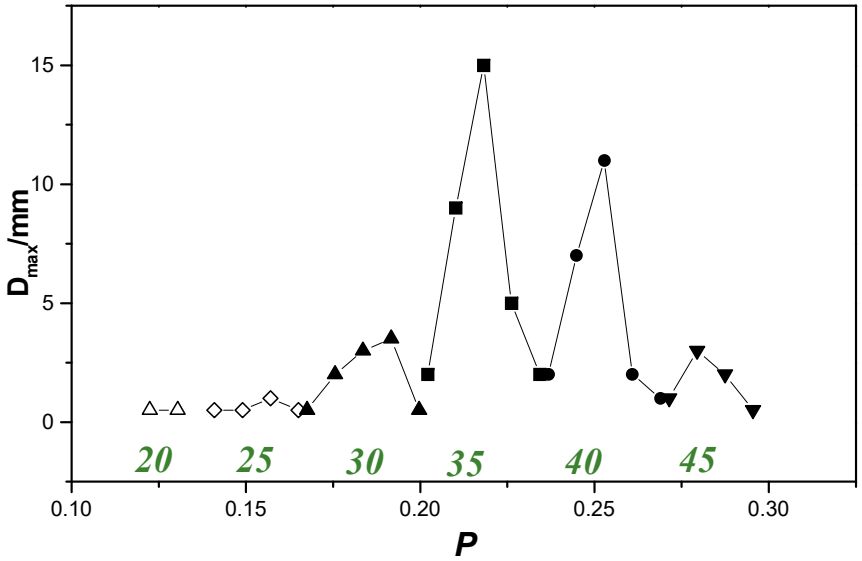

Similar trend of D_{max} with P

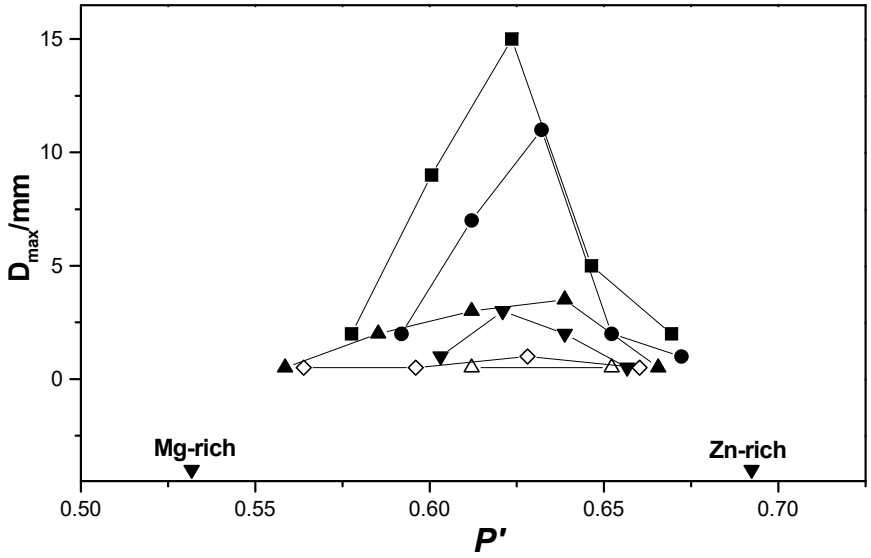

Maximum dia.(D_{max}) at P'=0.625

σ parameter (thermodynamic and atomic configuration aspects)

ΔT^* : Relative decrease of melting temp.

➡ liquid phase stability

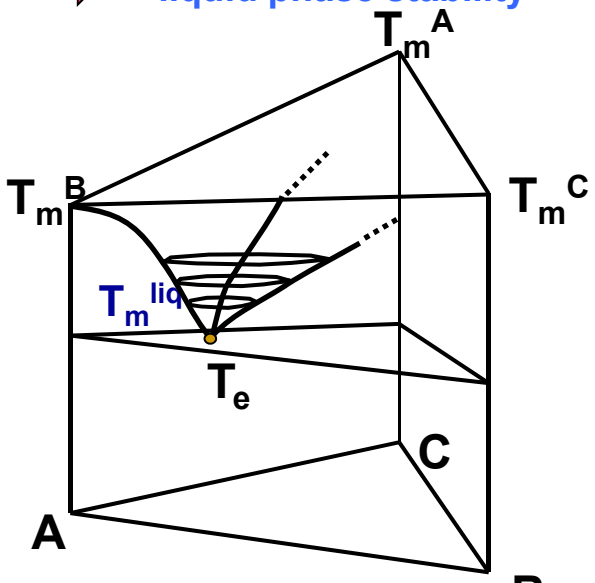

Deep eutectic condition

×

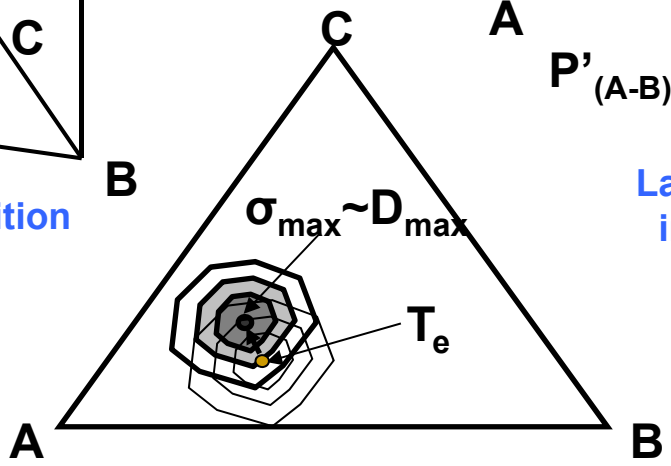

P' : Effective atomic mismatch per solute atom

➡ solid phase stability

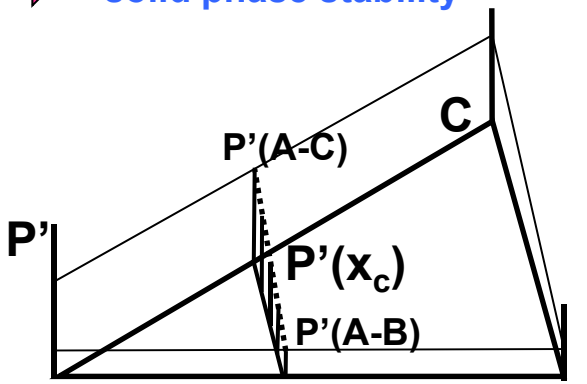

$P'_{(A-B)} \leq P'(Xc) \leq P'_{(A-C)}$

Large difference in atomic size

New criterion for GFA, σ parameter $\sigma = \Delta T^* \times P'$

* Appl. Phys. Lett., 86, 061907 (2005)

1) Calculation of GFA parameters in Ca-Mg-Zn alloy system

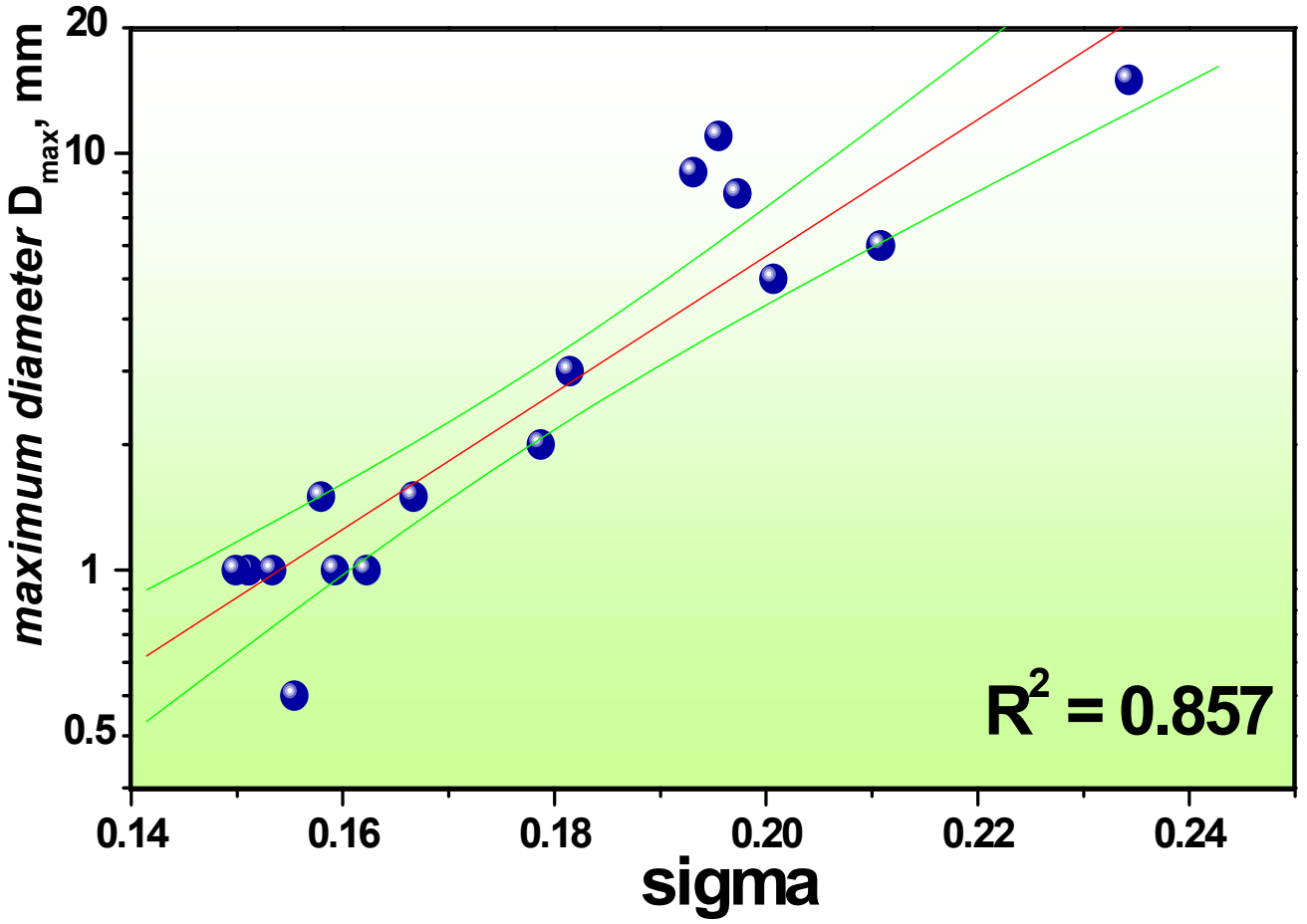

*** Sigma, σ parameter has a stronger correlation with GFA than other parameters suggested so far (ΔT_x: R^2=0.358, T_{rg}: R^2=0.787, K : R^2=0.607) in Ca-Mg-Zn alloy system.**

* J. Metastable and Nanocrystalline Materials, 24-25, 697 (2005)

2) Application of σ parameter for BMG-forming Ca-based ternary systems

Thermal analysis, GFA parameters and maximum diameter (D_{max}) for glass formation in the Ca-based ternary BMG systems

	T_g	T_x	T_l	T_l-T_g	ΔT_x	T_{rg}	K	γ	ΔT^*	σ	D_{max}
$Ca_{65}Mg_{15}Zn_{20}$	379	412	624	245	33	0.607	0.156	0.411	0.376	0.234	15
$Ca_{60}Mg_{25}Ni_{15}$	431	453	683	252	22	0.631	0.095	0.406	0.409	0.256	13
$Ca_{65}Mg_{20}Ag_{20}$	422	440	677	255	18	0.624	0.075	0.400	0.384	0.228	4
$Ca_{60}Al_{30}Mg_{10}$	449	474	709	260	24	0.634	0.103	0.409	0.318	0.201	2
$Ca_{60}Al_{30}Ag_{10}$	483	534	805	322	51	0.600	0.187	0.415	0.248	0.165	2
$Ca_{63}Al_{32}Cu_{5}$	512	523	831	320	11	0.615	0.037	0.389	0.221	0.150	2
$Ca_{60}Al_{30}Zn_{10}$	517	540	775	258	24	0.667	0.100	0.418	0.238	0.160	1.5
$Ca_{66.4}Al_{33.6}$	527	534	841	315	8	0.626	0.025	0.391	0.200	0.133	1

DSC traces for BMG-forming Ca-based ternary systems

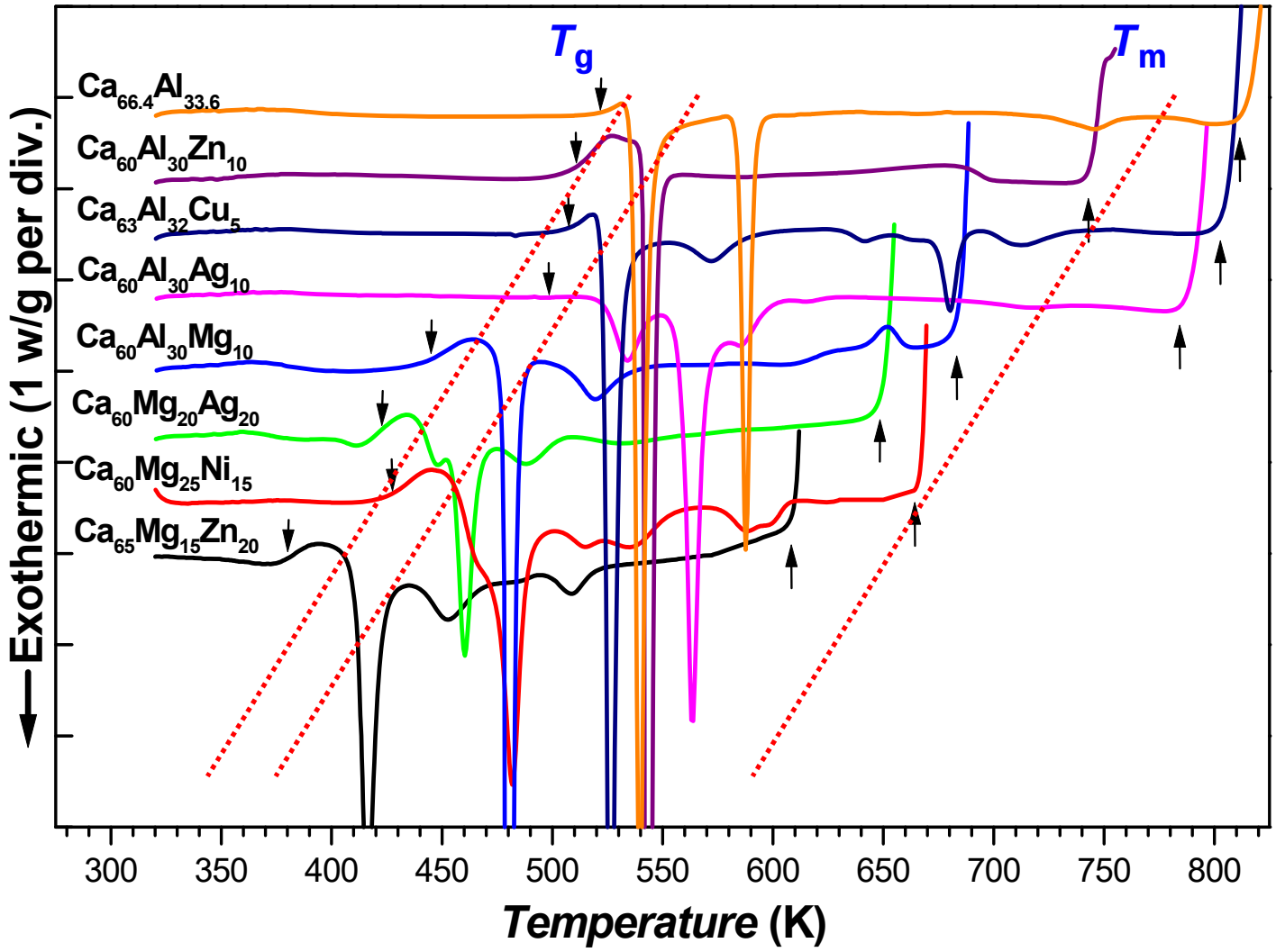

2) Calculation of GFA parameters in Ca-based BMG alloy systems

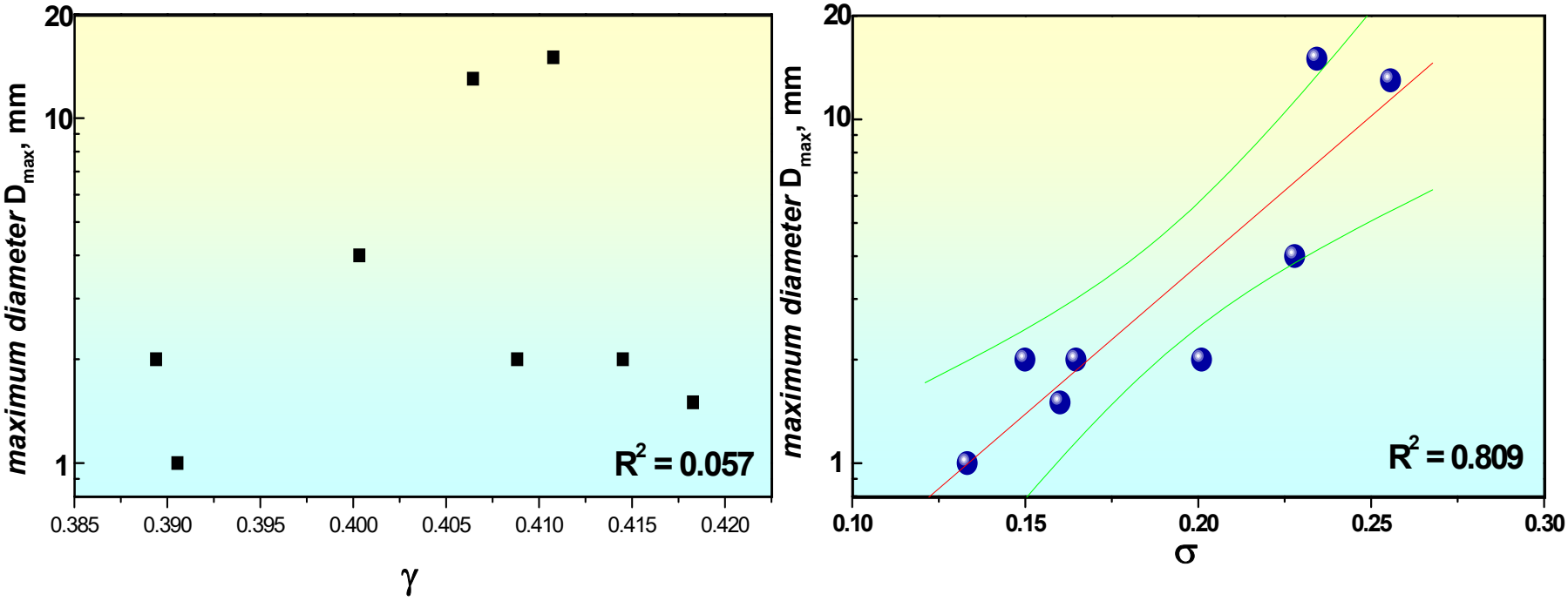

Sigma, σ parameter has a stronger correlation with GFA than other parameters suggested so far (ΔT_x: R^2=0.056, T_{rg}: R^2=0.080, K : R^2=0.148) in Ca-based BMG alloy systems.

* Appl. Phys. Lett. 86, 201912 (2005)

3) Application of σ parameter for BMG-forming ternary systems

Thermal analysis, GFA parameters and maximum diameter (D_{max}) for glass formation in the ternary BMG systems

	T_g	T_x	T_l	T_m^{mix}	ΔT_x	T_{rg}	K	γ	ΔT*	P'	σ	D_{max}
$Ca_{65}Mg_{15}Zn_{20}$	379	412	624	1032	33	0.607	0.156	0.411	0.395	0.624	0.234	15
$Nd_{60}Fe_{30}Al_{10}$	750	784	958	1385	34	0.783	0.195	0.459	0.308	0.620	0.199	15
$Pd_{40}Ni_{40}P_{20}$	590	671	991	1519	81	0.595	0.253	0.424	0.348	0.476	0.158	6
$Mg_{65}Cu_{25}Y_{10}$	425	486	720	1062	61	0.590	0.261	0.424	0.322	0.470	0.167	4
$Mg_{65}Ni_{20}Nd_{15}$	459	501	805	1076	42	0.571	0.139	0.397	0.252	0.504	0.148	3.5
$La_{55}Al_{25}Ni_{20}$	491	555	941	1226	64	0.521	0.166	0.388	0.232	0.623	0.148	3
$La_{55}Al_{25}Cu_{20}$	456	495	896	1166	39	0.509	0.097	0.366	0.231	0.613	0.139	3
$Pd_{73.5}Cu_{10}Si_{16.5}$	642	686	1128	1785	44	0.569	0.100	0.388	0.368	0.300	0.107	2

Calculation of G.F.A parameters

Ternary BMG system

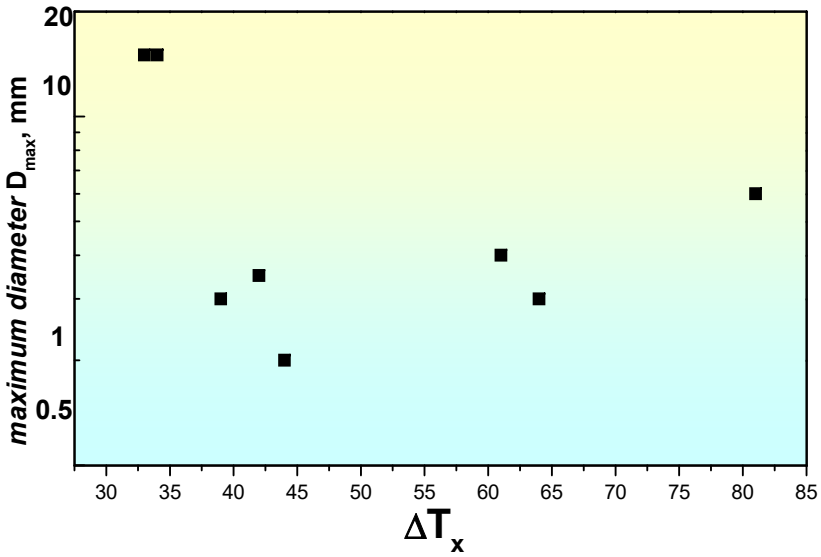

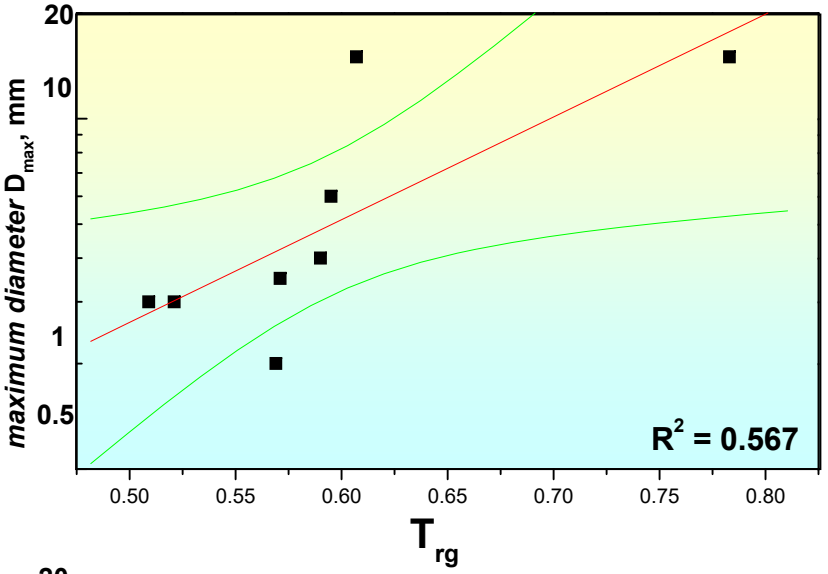

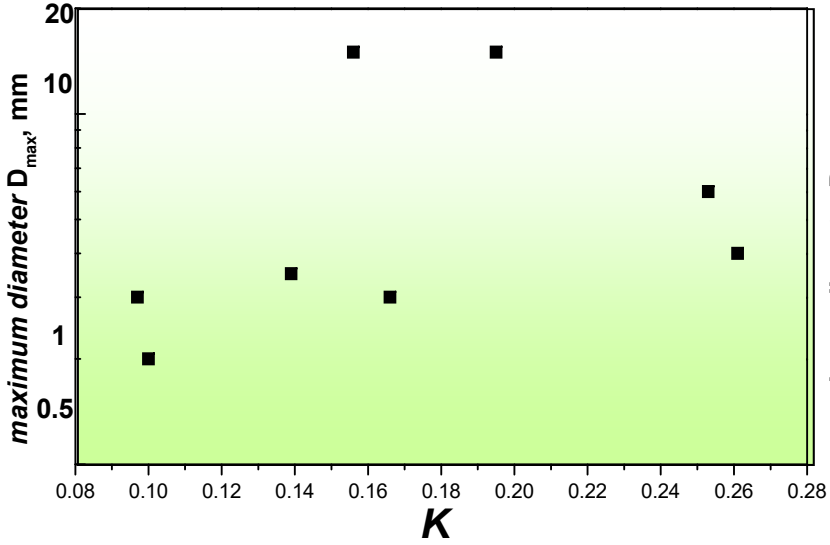

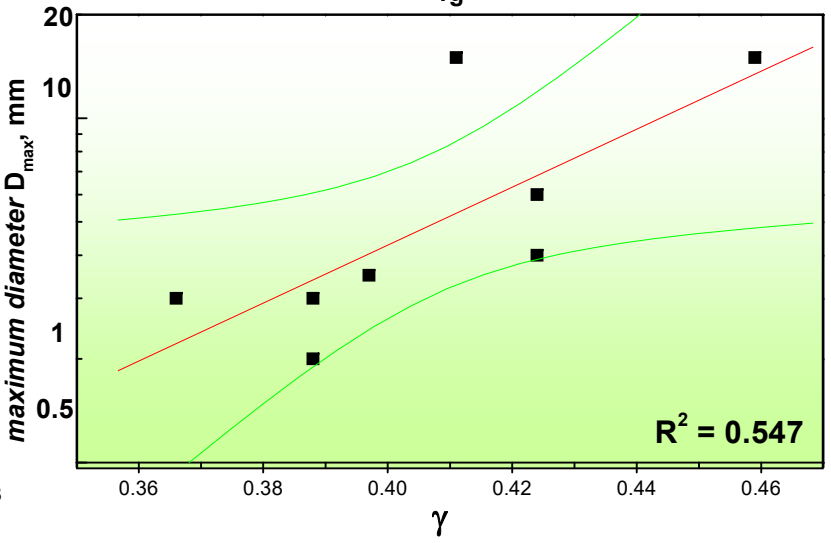

3) Calculation of GFA parameters in ternary BMG alloy systems

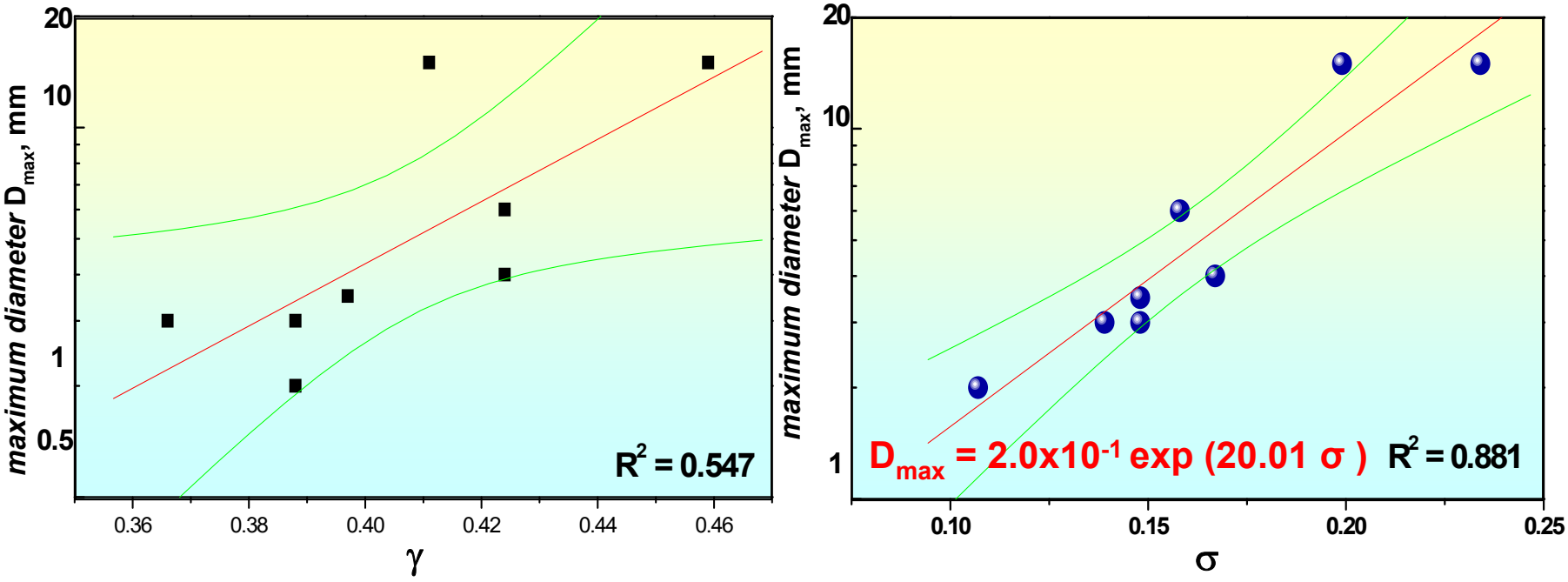

*** Sigma, σ parameter has a stronger correlation with GFA than other parameters suggested so far (ΔT_x: R^2=0.085, T_{rg}: R^2=0.567, K : R^2=0.136) in ternary BMG alloy systems.**

* Appl. Phys. Lett., 86, 061907 (2005)

Motivation for new criterion (1) : temperature range related with GFA parameters

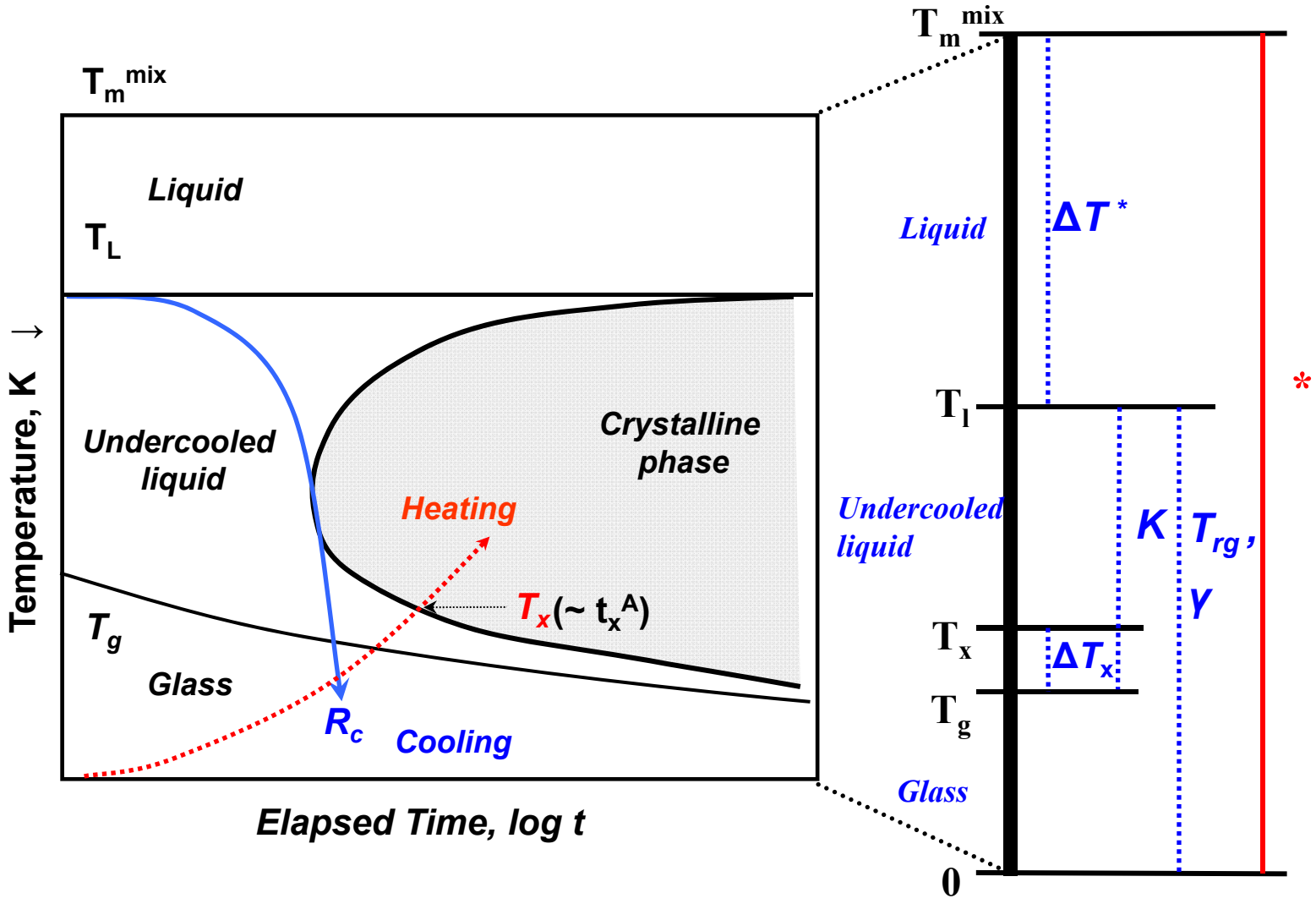

Motivation for new criterion (2) : Role of characteristic temp. for GFA

Positive Temperature Factor		Negative Temperature Factor
T_x	ΔT_x	T_g
T_g	T_{rg}	T_l
$T_m^{mix} - T_l$	ΔT^*	T_m^{mix}
ΔT_x	K	$T_l - T_x$
T_x	γ	$T_l + T_g$

With T_x ↑and T_l ↓, GFA parameter ↑. But, the role of T_g is not consistent.

Role of T_g with respect to GFA : Two different viewpoints

- from thermodynamic consideration

γ : stability of metastable liquid for glass formation

T_g ↓ ➡ GFA ↑

- Stability of the liquid during undercooling (i.e. metastable state, T_g)
: Liquid with lower Tg has the potential to be undercooled to lower temp., inducing its higher stability.

- from kinetic consideration

- constant cooling to temp. below Tg

$$X(T) = \frac{4\pi}{3R^4}\int_{T_l}^{T_g} I(T')\left[\int_{T'}^{T_g} U(T'')\mathrm{d}T''\right]^3 \mathrm{d}T'$$

X(T) : time dependent volume fraction of crystalline phase

If glass formation : $X<10^{-6}$

$$R_c^4 = \frac{4\pi}{3\times 10^{-6}}\int_{T_l}^{T_g} I(T')\left[\int_{T'}^{T_g} U(T'')\mathrm{d}T''\right]^3 \mathrm{d}T'$$

I & U = the steady-state nucleation frequency and the crystal growth rate

$$I = \frac{10^{35}}{\eta}\exp\left[\frac{-16\pi}{3}\cdot\frac{\Delta S_f^2 \alpha_m^3 T^2}{N_A k (T_l - T)^2}\right]$$

and

$$U = \frac{kT}{3\pi a^2 \eta}\left[1-\exp\left(-\frac{(T_l - T)\Delta S_f}{R_g T}\right)\right]$$

$1/R_c \propto$ increasing glass transition temp. Tg
viscosity of the supercooled liq.,
activation E for viscous flow, fusion entropy
decreasing liquidus temp. Tl

- T_{rg} : crystallization kinetics on GFA

T_g ↓ ➡ nucleation and growth rate ↑ -> GFA ↓

Points of issue for new GFA parameter

1. Combination of categories for glass formation

- γ parameter: thermodynamic/ kinetic aspects

➡ New parameter combining thermodynamic/ kinetic aspects

2. Temperature scale for GFA parameter

ΔT_x parameter : $T_x - T_g$

K parameter : $T_g - T_x - T_l$

T_{rg} parameter : $T_g - T_l$

γ parameter : $T_g - T_x - T_l$

ΔT^* parameter : $T_l - T_m^{mix}$

➡ New parameter covering temperature range $T_g - T_x - T_l - T_m^{mix}$ with considering about two different role of T_g

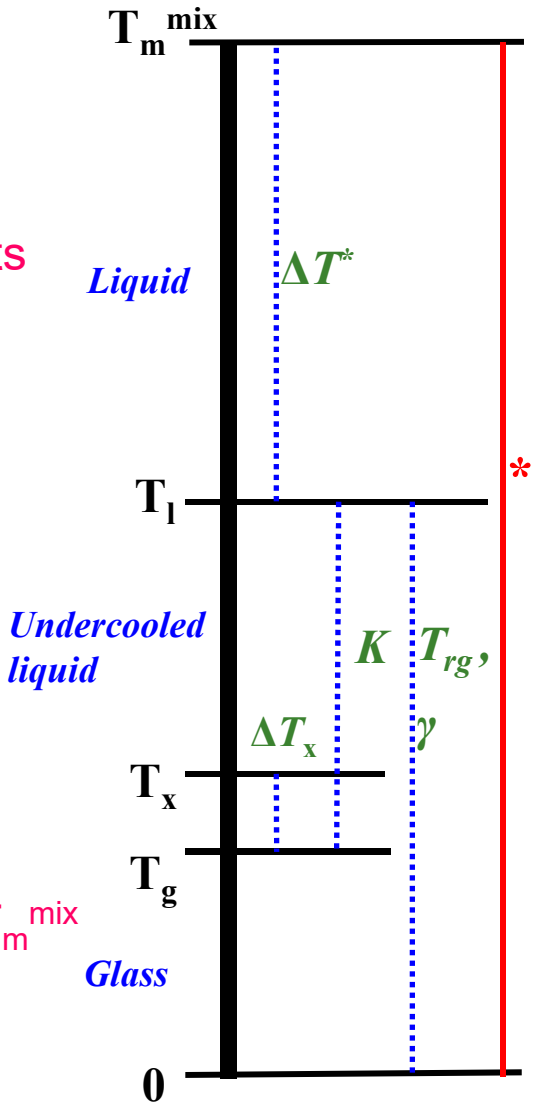

$$\mathrm{GFA} \propto (\Delta T_m, \Delta T_x, T_x).$$

As discussed above, in evaluating the GFA, the thermodynamic stability of the liquid phase should be considered. The stability of the liquid phase can be considered in two states, i.e., equilibrium state (above T_l) and the metastable state (T_l–T_g). The effect of the stability of liquid at equilibrium state on GFA can be reflected by considering the relative depression of T_l. To reflect the degree of relative depression of T_l, T_m^{mix} can be utilized as a departure of the alloy liquidus temperature from the rule of mixtures liquidus temperature.[8] Although T_m^{mix} is an imaginary temperature, it can be calculated from melting points and composition of the constituent elements, thereby being able to effectively reflect the compositional effects on the depression of T_l as used in the ΔT^* parameter. Therefore, the temperature range between T_m^{mix} and T_l ($=\Delta T_m$) can be used as a temperature factor reflecting the stability of stable liquid.

$$\mathrm{GFA} \propto (\Delta T_m, \Delta T_x, T_x).$$

The effect of the stability of liquid at metastable state on GFA can be reflected by considering the relative depression of T_g. From the thermodynamic point of view, T_g as a temperature factor is expected to play an important role in evaluating the GFA. However, if T_g is directly included as the temperature factor in the GFA parameter, it creates a conflict in the fractional expression of GFA parameter because the stability of the liquid in metastable state increases with a decrease in T_g but the nucleation and growth rate also increase with a decrease in T_g. Thus, the stability of the liquid at metastable state (i.e., glass phase) is reflected by ΔT_x instead of T_g. Although ΔT_x alone is not sufficient to represent the GFA, ΔT_x can resolve the contradiction of T_g as one of the temperature factors in the GFA parameter, reflecting the stability of undercooled liquid.

$$\mathrm{GFA} \propto (\Delta T_m,\ \Delta T_x,\ T_x).$$

In principle, the kinetic aspect for glass formation would better be approached by considering how liquid can easily avoid the nucleation and growth of the crystalline phase during cooling as considered in T_{rg}. However, as mentioned above, directly, including T_g can cause some vagueness in evaluating the GFA. Thus, we consider kinetic resistance to crystallization of the glass state by the quantity of T_x,[38] because it is possible to determine the lower part of crystallization curve (C curve) in CCT diagram from rate dependent thermal analysis upon reheating of the glass samples. The glass with higher T_x can be regarded to exhibit longer time for onset of crystallization, i.e., higher resistance to crystallization. Therefore, T_x can be used as one of the temperature factors, reflecting resistance to crystallization of the glass phase.

A new criterion for GFA : ε parameter

a. Liquid phase stability :

- Relative stability of stable liquid : distance from the T_m^{mix} to liquidus melting temp.,

$$\Delta T_m = T_m^{mix} - T_l \qquad (\gamma \text{ parameter: } T_l)$$

- Stability of metastable liquid : range of supercooled liquid,

$$\Delta T_x = T_x - T_g \qquad (\gamma \text{ parameter: } T_g)$$

b. Resistance to crystallization : T_x (γ parameter: T_x)

- relative difficulties for the formation (nucleation and crystal growth)

  of the competing crystalline phases in various BMG forming alloy system

- Retarding incubation time for crystallization : relative position of the CCT curves along the time axis

c. nomalizing : T_m^{mix}

- Exclusion of systematic and compositional effects in various BMG alloy systems

A New criterion for GFA of BMGs

$$\varepsilon = \frac{\Delta T_m + \Delta T_x + T_x}{T_m^{mix}}$$

E. S. Park et al., *JAP (2015)*

ε parameter (thermodynamic and kinetic aspects)

A New criterion for GFA of BMGs

$$\varepsilon = \frac{\Delta T_m + \Delta T_x + T_x}{T_m^{mix}}$$

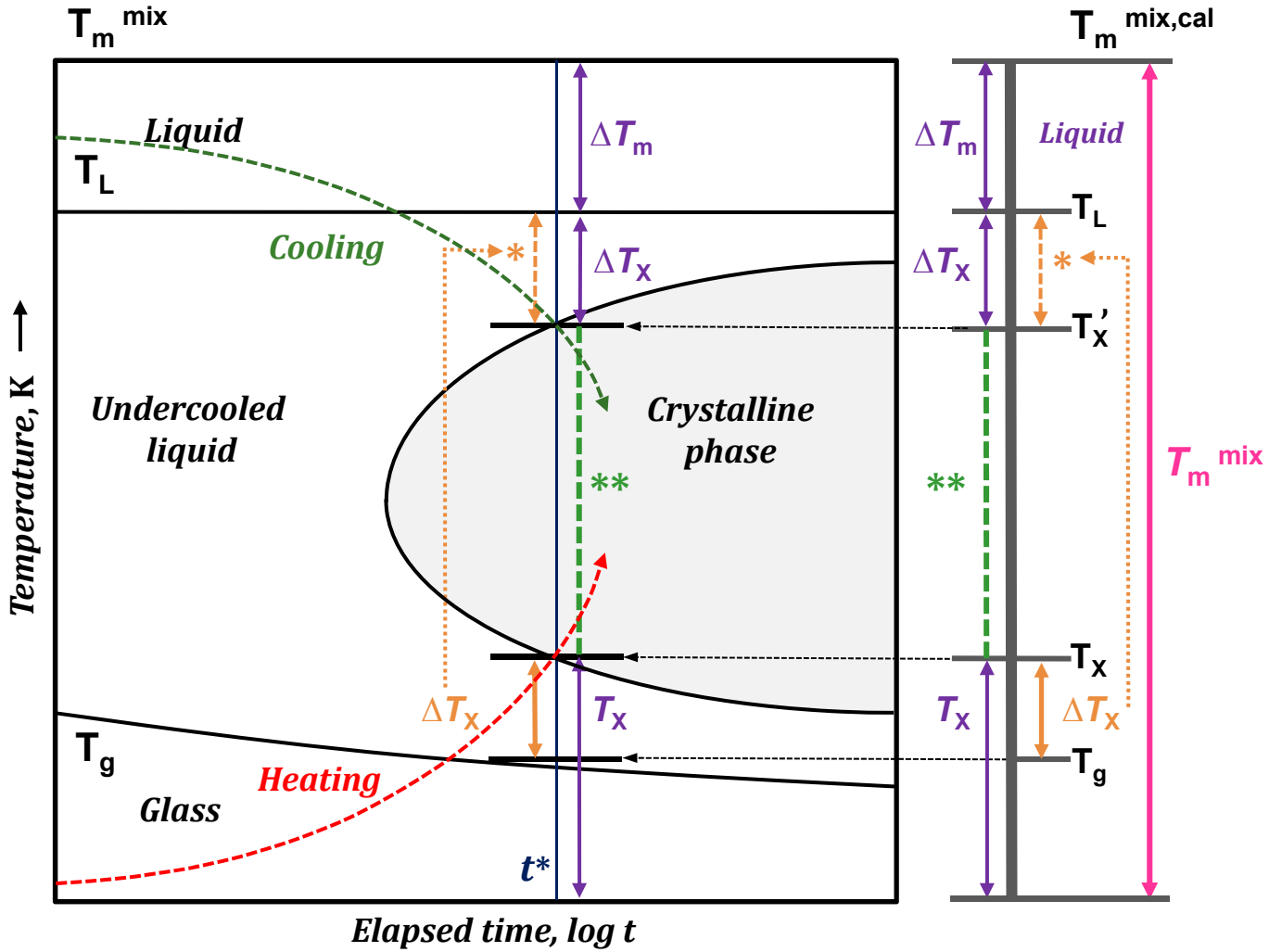

ε parameter (thermodynamic and kinetic aspects)

A New criterion for GFA of BMGs

$$\varepsilon = \frac{\Delta T_m + \Delta T_x + T_x}{T_m^{mix}}$$

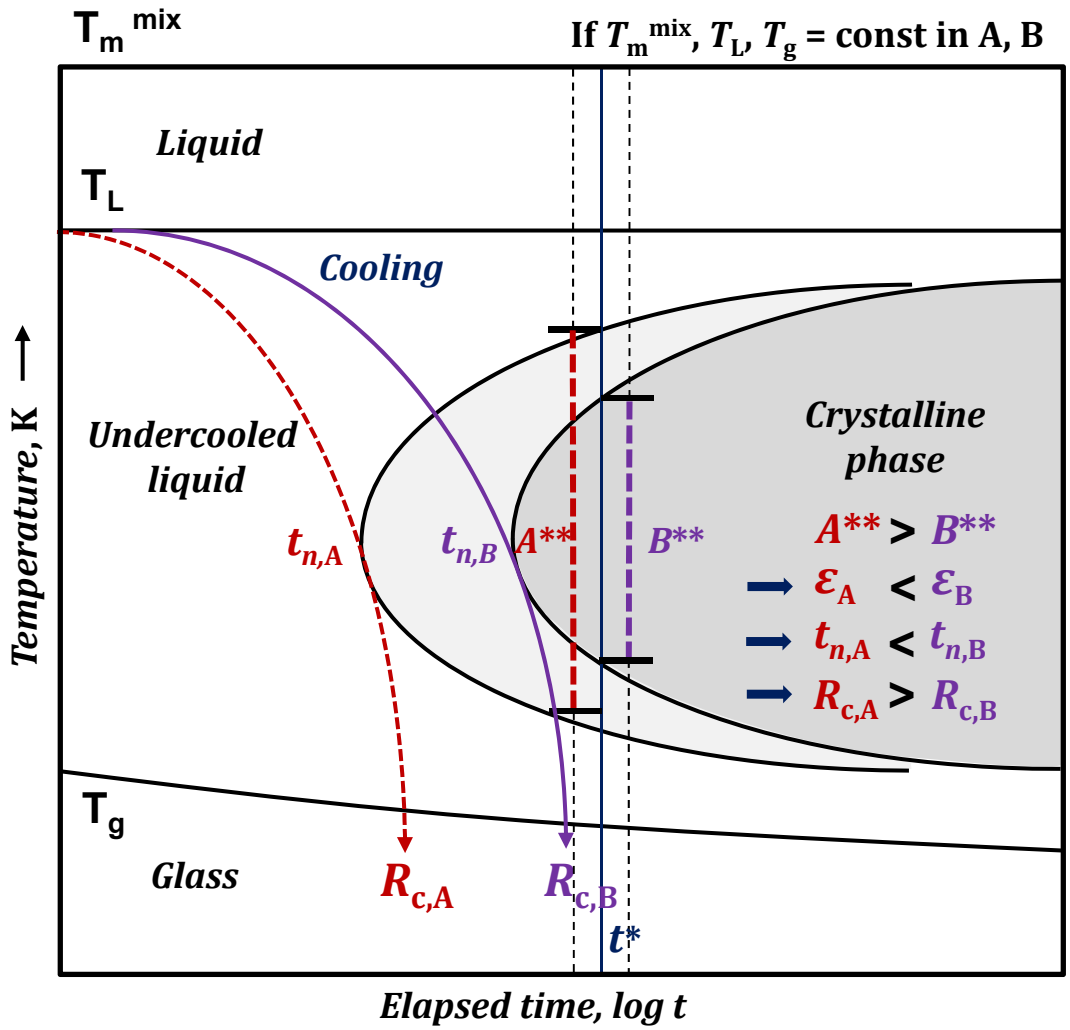

ε parameter (thermodynamic and kinetic aspects)

A New criterion for GFA of BMGs

$$\varepsilon = \frac{\Delta T_m + \Delta T_x + T_x}{T_m^{mix}}$$

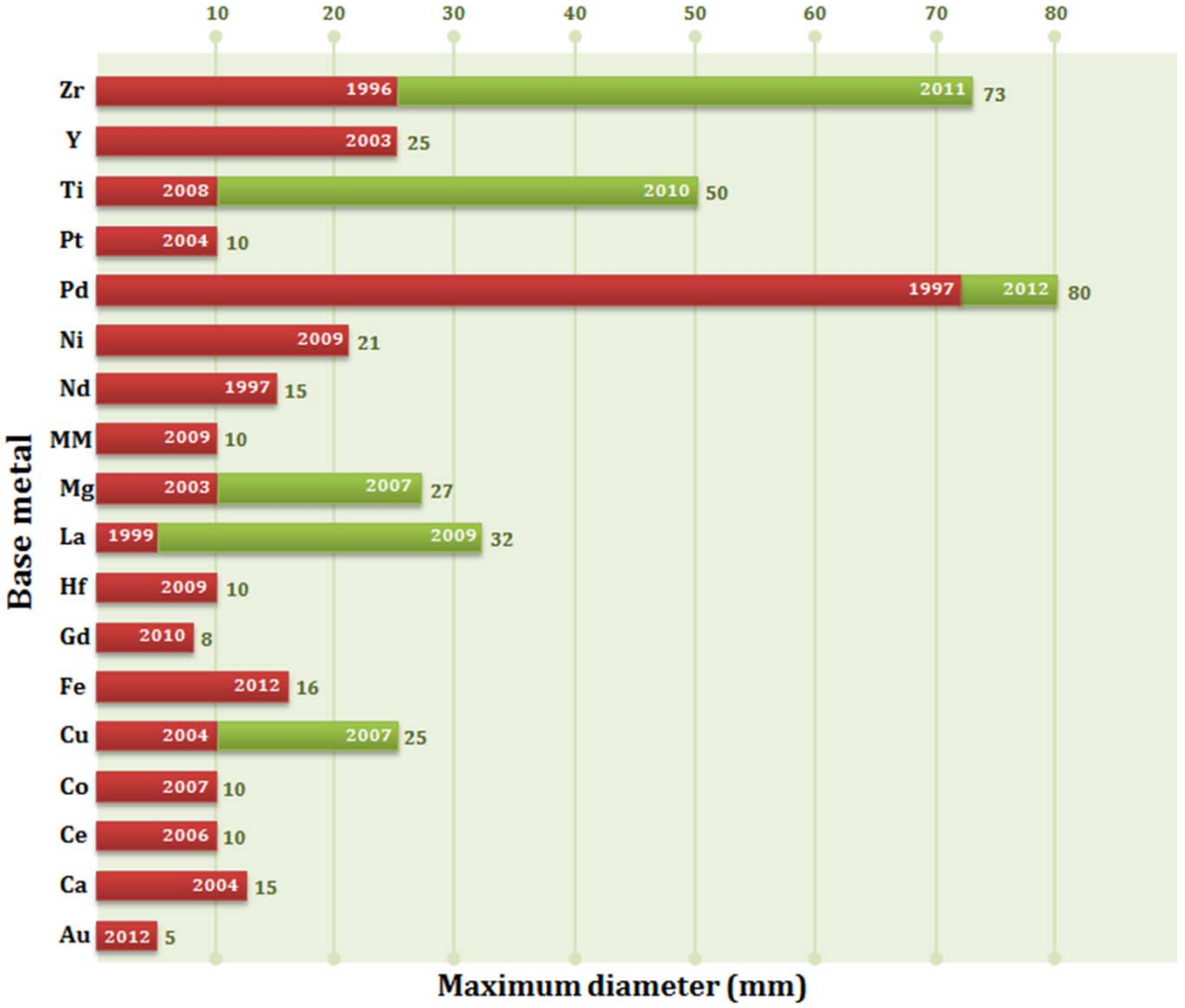

TABLE III. Results of thermal analysis, Z_{max}, and R_c for the various BMG-forming alloy systems, including the data for some conventional metallic glasses previously reported.

Alloy	T_g (K)	T_x (K)	T_l (K)	T_m^{mix} (K)	Z_{max} (mm)	R_c (K/s)	References
Ge	750	750	1210	1210	…	5.0×10^5	Ref. 39
Ni	425	425	1725	1725	…	3.0×10^{10}	Ref. 39
Te	290	290	723	723	…	3.2×10^6	Ref. 39
$Au_{55}Cu_{25}Si_{20}$	348	383	654	1412	0.5	…	Ref. 40
$Au_{46}Ag_5Cu_{29}Si_{20}$	395	420	664	1408	1	…	Ref. 40
$Au_{52}Pd_{2.3}Cu_{29.2}Si_{16.5}$	393	427	651	1412	2	…	Ref. 40
$Au_{49}Ag_{5.5}Pd_{2.3}Cu_{26.9}Si_{16.3}$	401	459	644	1405	5	…	Ref. 40
$Ca_{66.4}Al_{33.6}$	527	534	841	1052	1	…	Ref. 41
$Ca_{63}Al_{32}Cu_5$	512	523	831	1067	2		Ref. 41
$Ca_{60}Mg_{25}Ni_{15}$	431	453	683	1157	13	24	Ref. 34
$Ca_{65}Mg_5Zn_{30}$	382	414	743	977	1	…	Ref. 42
$Ca_{65}Mg_{10}Zn_{25}$	378	414	686	988	6	…	Ref. 42
$Ca_{65}Mg_{15}Zn_{20}$	379	412	624	1000	15	20	Refs. 42 and 43
$Ce_{70}Al_{10}Cu_{20}$	341	408	722	1112	2	…	Ref. 44
$Ce_{68}Al_{10}Cu_{20}Fe_2$	352	423	708	1127	5	…	Ref. 44
$Ce_{68}Al_{10}Cu_{20}Nb_2$	345	421	721	1146	8	…	Ref. 44
$Ce_{68}Al_{10}Cu_{20}Co_2$	352	419	716	1126	10	…	Ref. 44
$Co_{75}Si_{15}B_{10}$	785	785	1393	1815		3.5×10^5	Ref. 39
$Co_{40}Fe_{22}Nb_6Zr_2B_{30}$	903	1000	1585	2022	1	…	Ref. 47
$Co_{43}Fe_{20}Ta_{5.5}B_{31.5}$	910	982	1492	2048	2	…	Refs. 45 and 46
$Co_{48}Cr_{15}Mo_{14}C_{15}B_6$ Er_2	848	933	1394	2345	10	…	Ref. 48

Cu-based

Cu-Zr

Cu-Zr-Al

Cu-Zr-Al-Al

Cu-Zr-Al-Y

Cu-Zr-Ti

Cu-Zr-Ti-Be

Cu-Zr-Ti-Ni-(Si,Sn)

Fe-based

Fe-B

Fe-Ni-B

Fe-Si-B

Fe-P-C

Fe-Nb-Y-B

Fe-Cr-Mo-C-B-(Y)

Mg-based

Mg-Ni-Nd

Mg-Cu-Y-(Ag)

Mg-Cu-Gd-(Ag)

Mg-Cu-Ag-Pd-Gd

Mg-Cu-Ni-Zn-Ag-Y-(Gd)

Ni-based

Ni-Nb

Ni-Nb-Ta

Ni-Nb-Ti-Hf

Ni-Si-B

Ni-Zr-Ti-(Sn-Si)

Ni-Zr-Ti-Si-Sn-Nb

Zr-based

Zr-Al-Ni

Zr-Al-Cu-Ni

Zr-Al-Cu-Ni-Ti

Zr-Be-Cu-Ni-Ti

Ca-based

Ca-Al

Ca-Al-Cu

Ca-Mg-Ni

Ca-Mg-Zn

Co-based

Co-Si-B

Co-Fe-Ta-B

Co-Fe-Nb-Zr-B

Nd-based

Nd-Al-Fe

Nd-Al-Ni-Cu-Co

Nd-Al-Ni-Cu-Fe

La-based

La-Al-Ni

La-Al-Cu

La-Al-Ni-Cu

La-Al-Ni-Co-Cu

Y-based

Y-Al-Co

Y-Al-Co-Sc

Y-Al-Co-Ni-Sc

Pt-based

Pt-Ni-P

Pt-Cu-Ni-P

Pt-Cu-Co-P

Pd-based

Pd-Si

Pd-Cu-Si

Pd-Ni-P

Pd-Cu-Ni-P

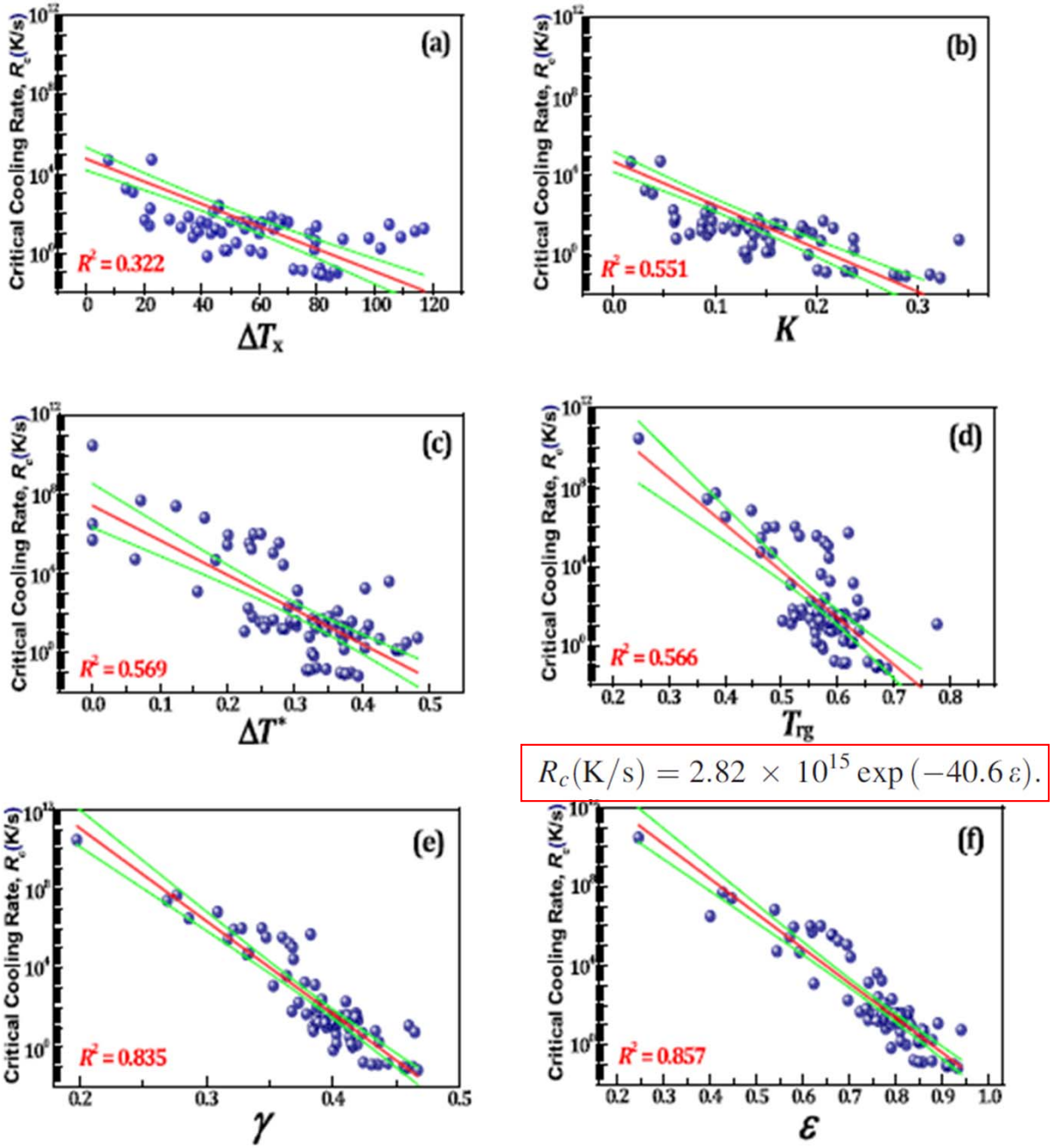

FIG. 4. A correlation between the parameters for GFA (ΔT_x, K, T_{rg}, ΔT^*, γ, and ε parameters) and R_c for the various glass-forming alloy systems reported previously.

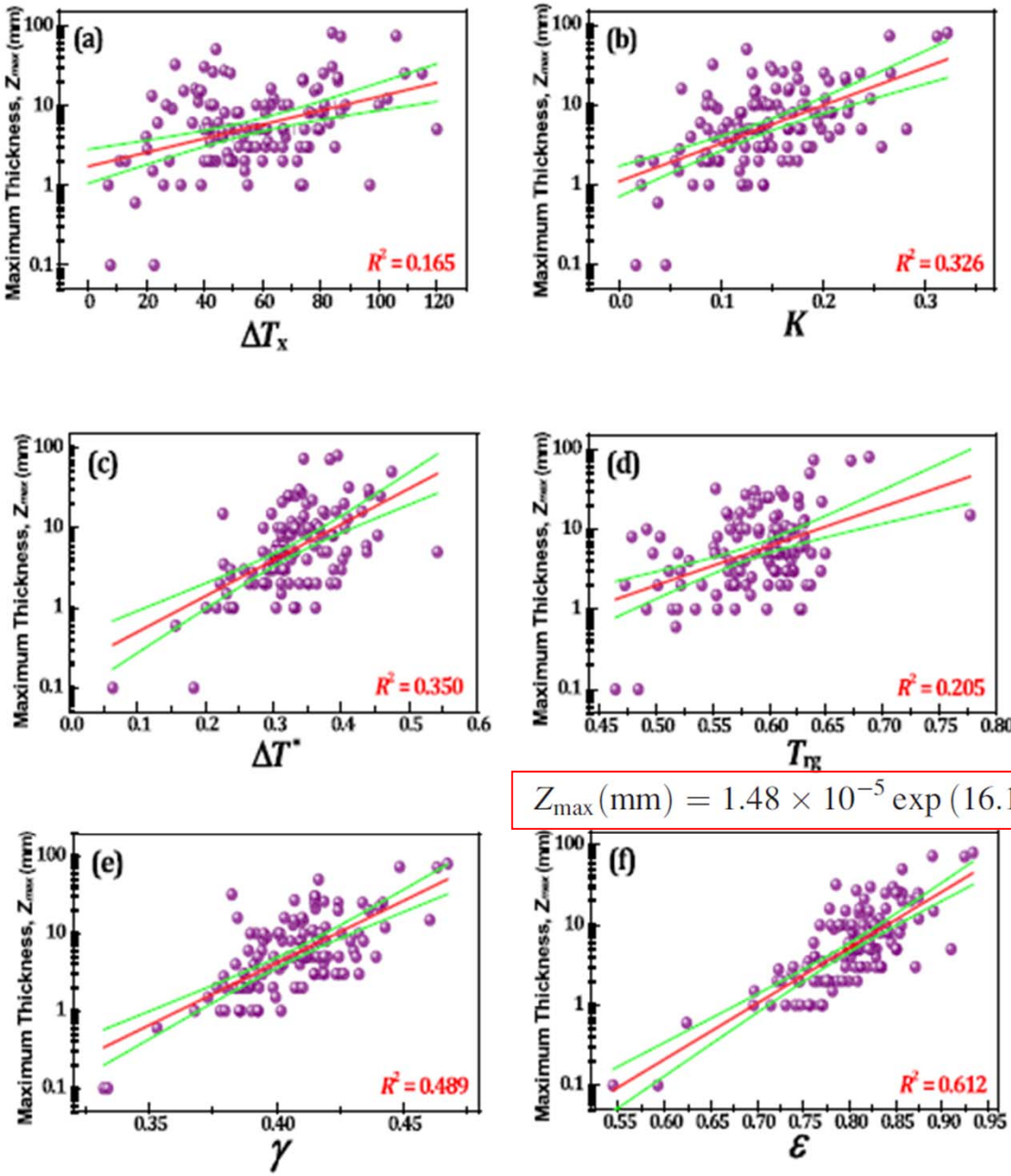

FIG. 5. A correlation between the parameters for GFA (ΔT_x, K, T_{rg}, ΔT^*, γ, and ε parameters) and Z_{max} for the various BMG-forming alloy systems reported previously.

$$R_c(\mathrm{K/s}) = 2.82 \times 10^{15} \exp(-40.6\,\varepsilon).$$

$$Z_{\max}(\mathrm{mm}) = 1.48 \times 10^{-5} \exp(16.1\,\varepsilon).$$

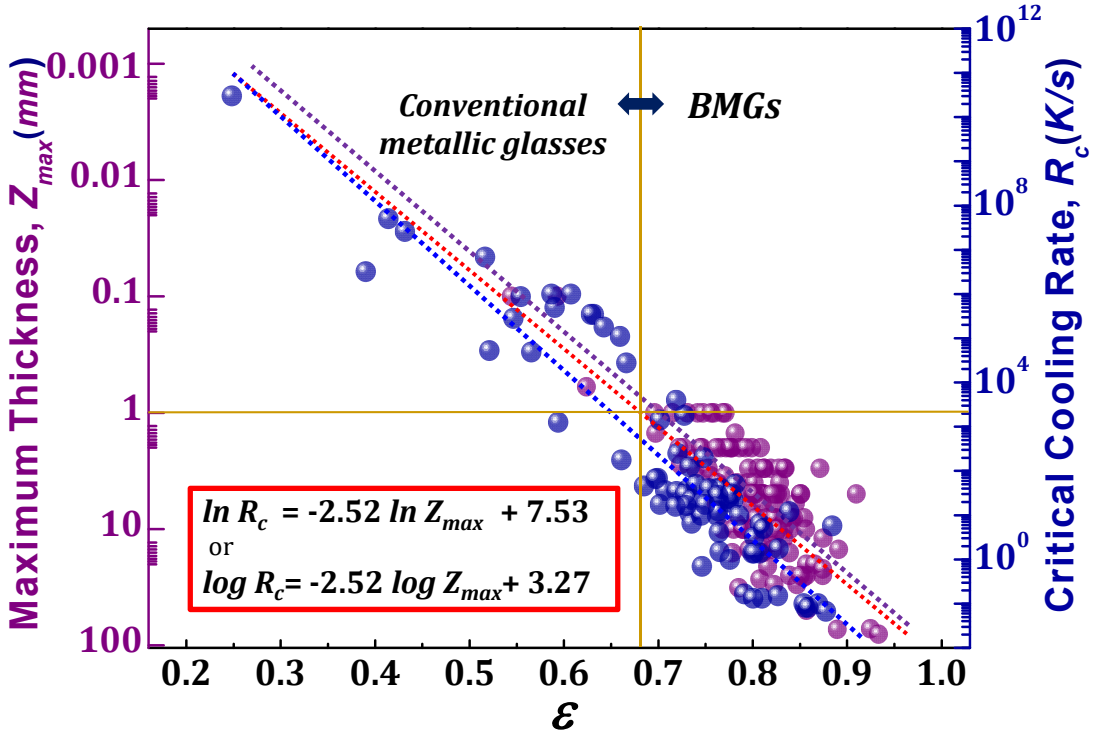

$$R_c = 2.82 \times 10^{15} \exp(-40.6\,\varepsilon)$$

or

$$Z_{\max} = 1.48 \times 10^{-5} \exp(16.1\,\varepsilon).$$

Improvement of GFA

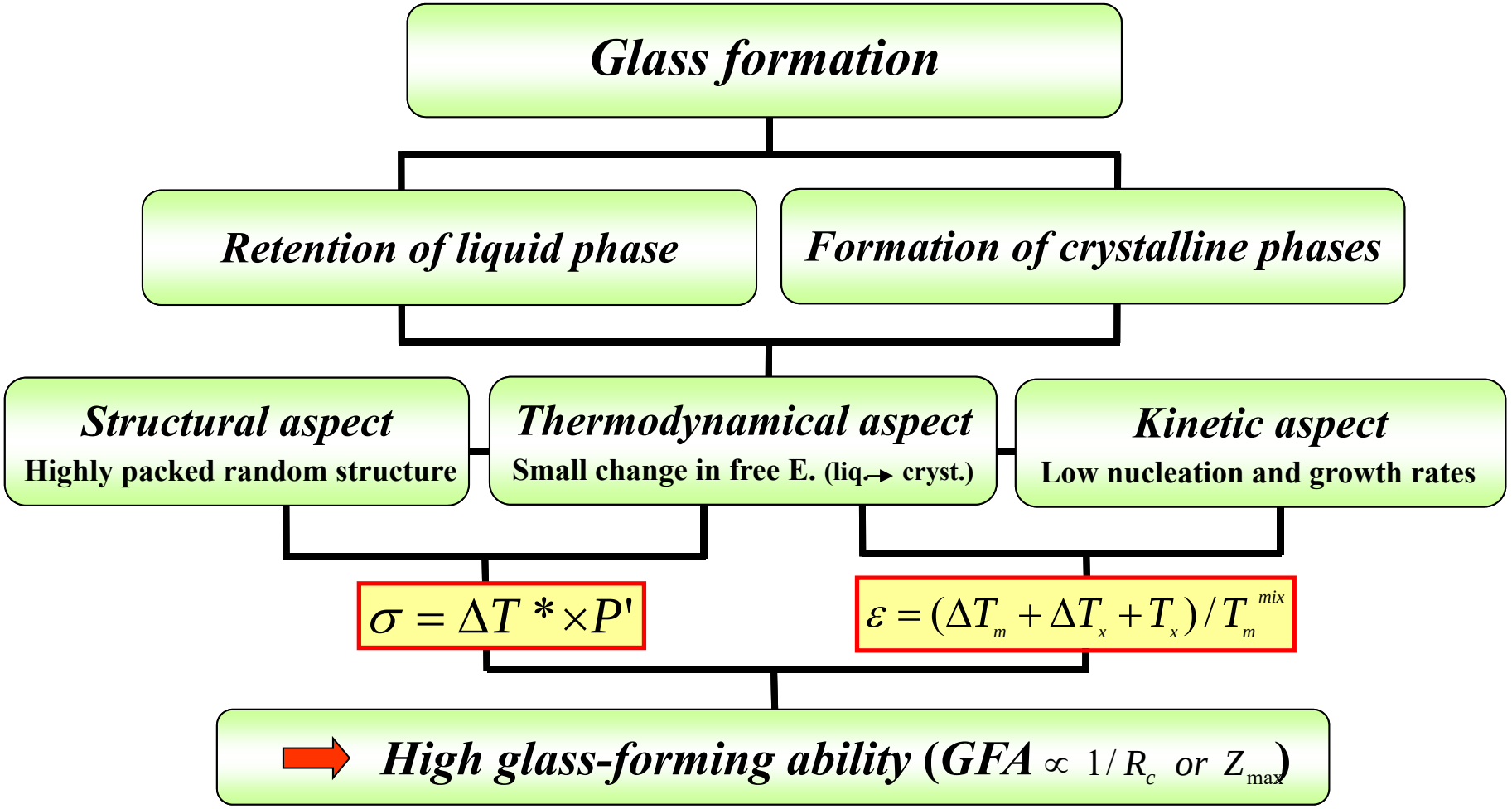

In estimating the GFA, the combinational effects of thermodynamic, kinetic and structural aspects for glass formation should be considered.

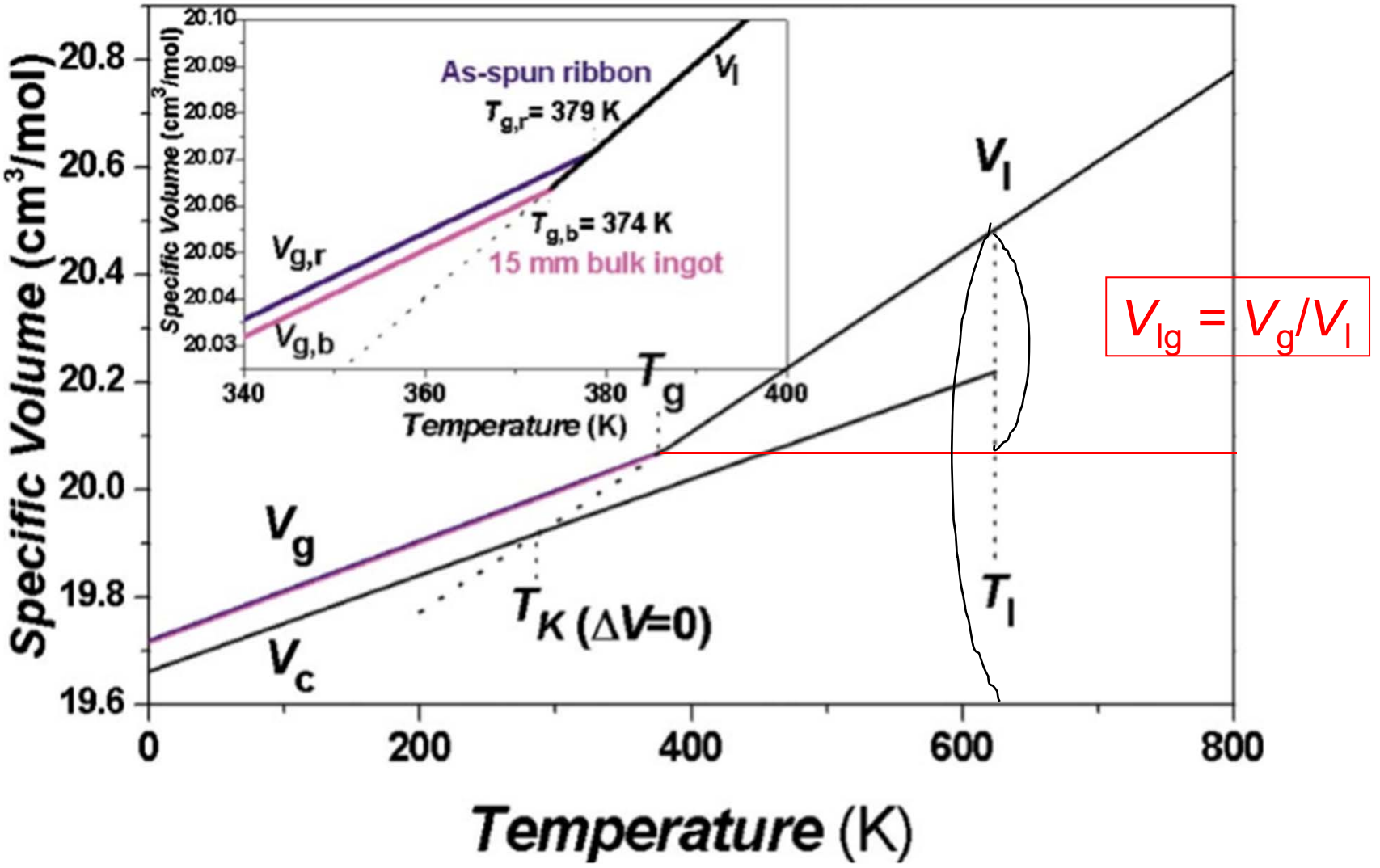

FIG. 1. (Color online) Specific volume as a function of temperature in the liquid V_l, glass V_g, and crystalline V_c of $Ca_{65}Mg_{15}Zn_{20}$ alloy.

TABLE I. Summaries of thermal analysis (T_g and T_l), V_g, V_l, β_l/T_l, T_{rg}, V_{lg}, and R_c for various MGAs.

Composition	T_g (K)	T_l (K)	V_g (cm^3/g)	V_l (cm^3/g)	β_l/T_l ($\times 10^{-8}$)	T_{rg}	V_{lg}	R_c (K/s)
$Pd_{43}Cu_{27}Ni_{10}P_{20}$	576	845	0.108	0.110	7.999	0.682	0.018	0.01
$Pd_{40}Ni_{40}P_{20}$	583	974	0.108	0.111	7.097	0.599	0.027	0.167
$Zr_{41.2}Ti_{13.8}Cu_{12.5}Ni_{10}Be_{22.5}$	623	996	0.163	0.167	6.447	0.626	0.024	1.40
$Zr_{57}Cu_{15.4}Ni_{12.6}Al_{10}Nb_5$	682	1115	0.147	0.150	4.143	0.612	0.020	10
$Zr_{55}Al_{22.5}Co_{22.5}$	753	1323	0.162	0.167	4.376	0.569	0.033	17.5
$Ca_{65}Mg_{15}Zn_{20}$	379	624	0.469	0.479	13.66	0.607	0.021	20
$Zr_{52.5}Cu_{17.9}Ni_{14.6}Al_{10}Ti_5$	675	1090	0.152	0.156	5.668	0.619	0.026	25
$Cu_{46}Zr_{42}Al_7Y_5$	675	1123	0.147	0.151	5.663	0.601	0.028	40
$Ni_{59.5}Nb_{40.5}$	920	1448	0.116	0.120	4.360	0.635	0.033	250
$Pd_{77.7}Cu_6Si_{16.5}$	653	1015	0.096	0.099	8.247	0.643	0.030	320
$Cu_{50}Zr_{50}$	670	1219	0.134	0.139	5.363	0.550	0.036	1000
$Pd_{82}Si_{18}$	629	1071	0.095	0.098	6.467	0.587	0.031	1800
$Ni_{80}P_{20}$	618	1192	0.128	0.134	6.544	0.518	0.045	1.0×10^5
Ge	750	1210	0.174	0.182	7.897	0.620	0.044	5.0×10^5
Te	290	723	0.163	0.172	16.71	0.401	0.052	3.2×10^6

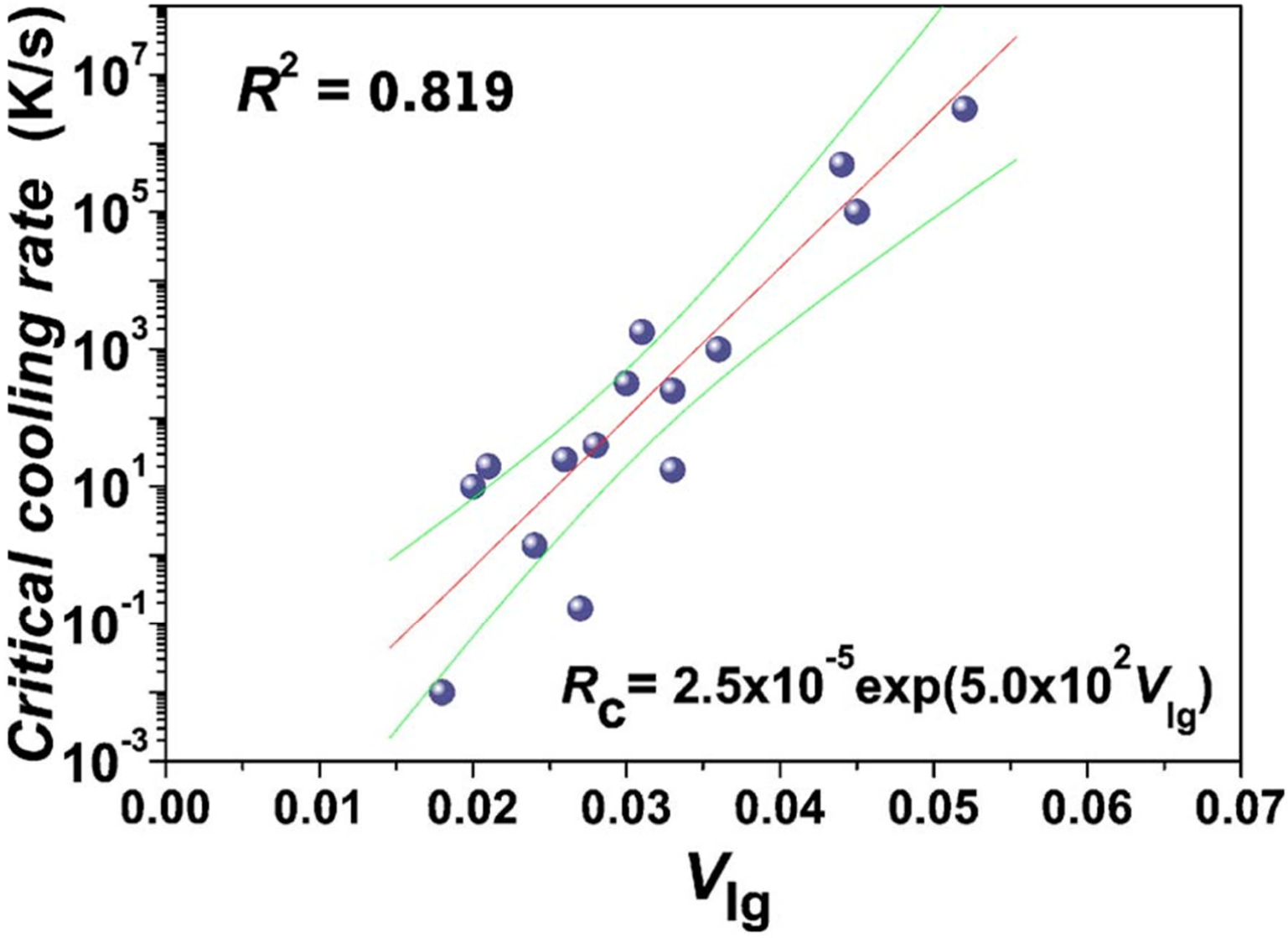
Critical cooling rate (K/s)
10^{7}
10^{5}
10^{3}
10^{1}
10^{-1}
10^{-3}
R^2 = 0.819
R_c= 2.5x10^{-5}exp(5.0x10^{2}V_{lg})
0.00
0.01
0.02
0.03
0.04
0.05
0.06
0.07
V_{lg}

$$\mathrm{GFA} \propto (\varepsilon,\ V_{epsilon} = \frac{V(T_m^{mix} - T_l) + V(T_x - T_g) + V(T_x)}{V(T_m^{mix})})$$

$$\kappa = (1-\varepsilon)\times(1-V_\varepsilon)$$

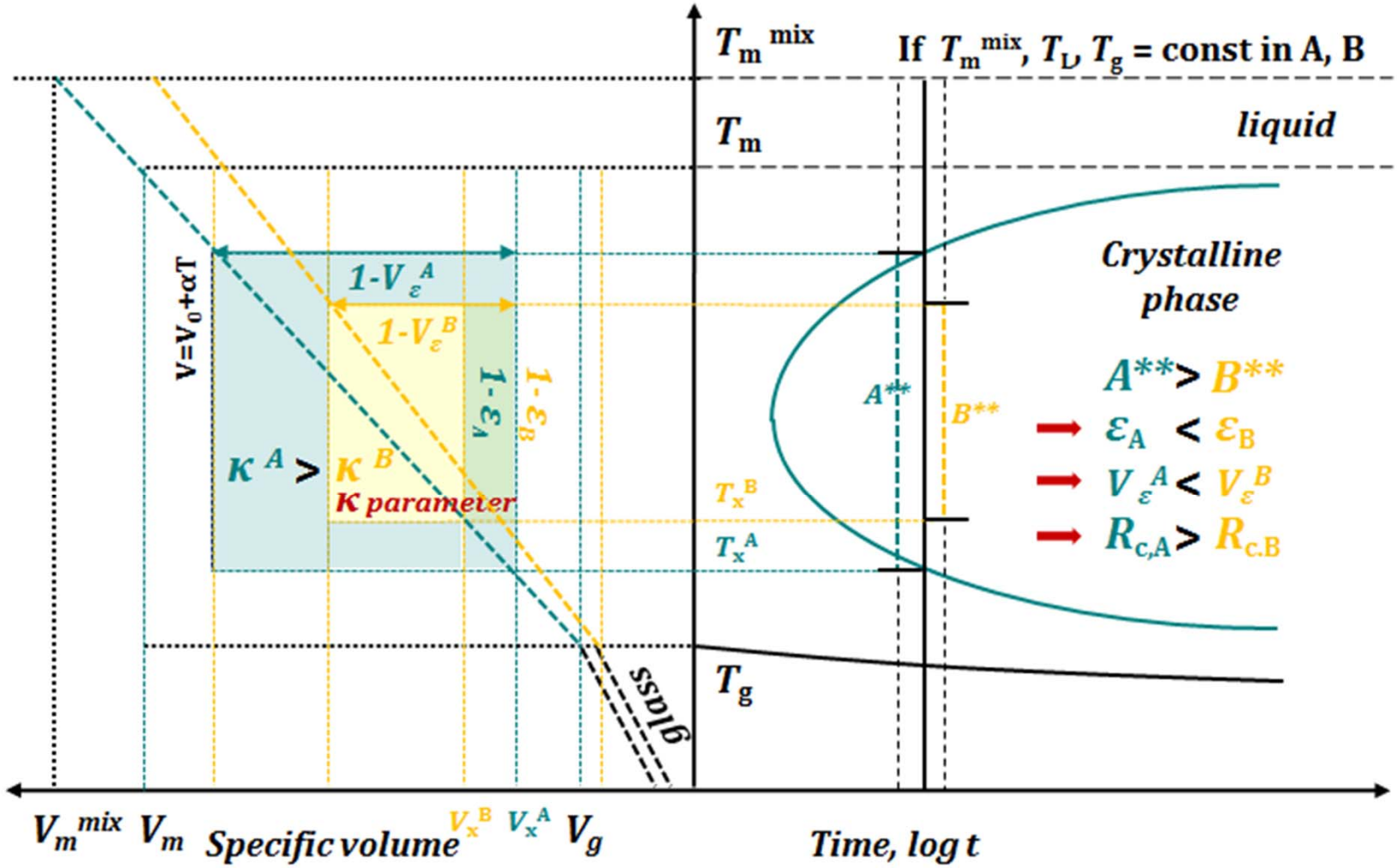

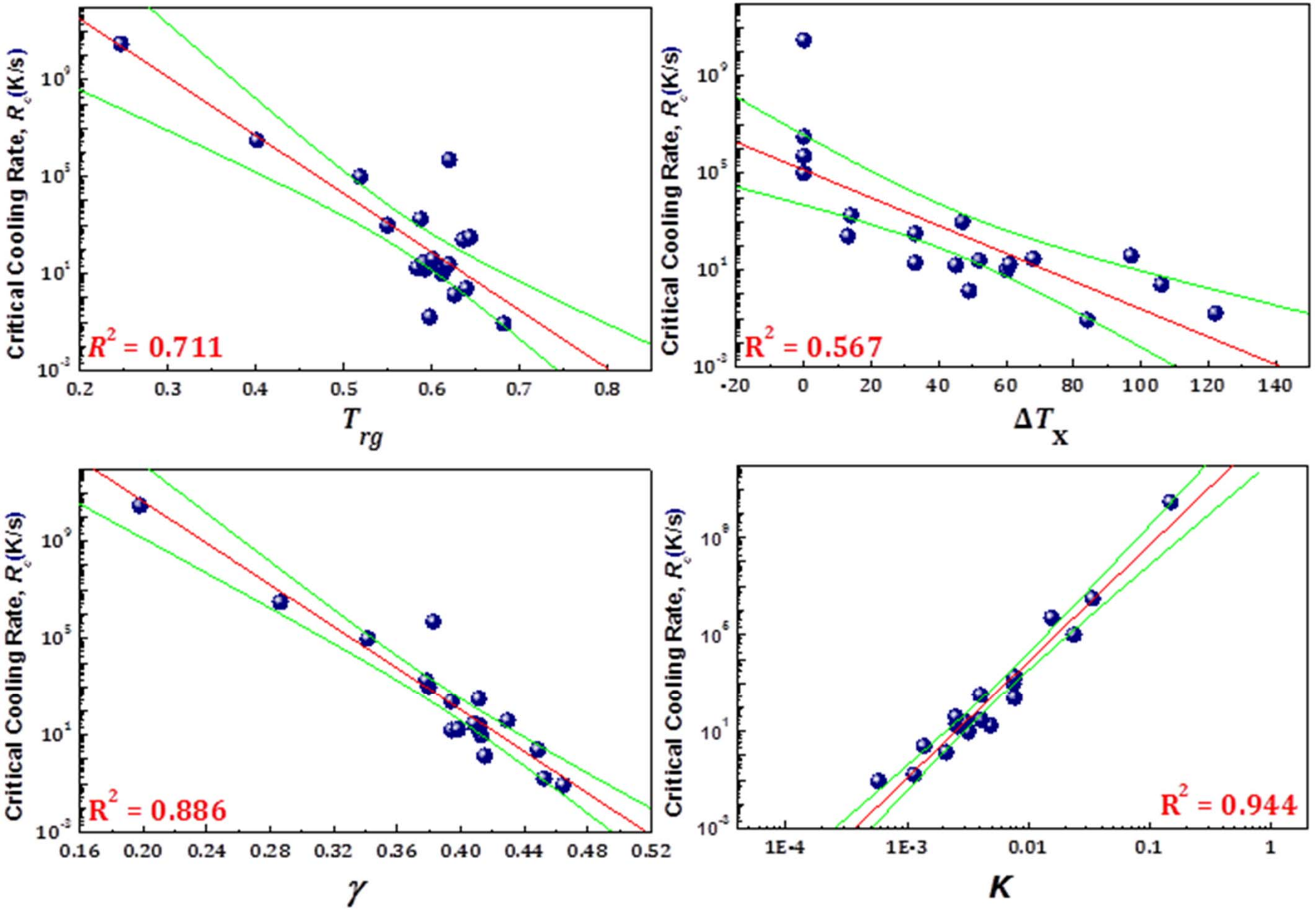
Critical Cooling Rate, R_c(K/s)
R^2 = 0.711
T_{rg}
Critical Cooling Rate, R_c(K/s)
R^2 = 0.567
ΔT_x
Critical Cooling Rate, R_c(K/s)
R^2 = 0.886
γ
Critical Cooling Rate, R_c(K/s)
R^2 = 0.944
K

IH4: Explain the detail how to get R^2 (regression coefficient) during fitting.

IH5: Please make a summary of other GFA parameters based on termo-dynamic modeling, structural and topological parameters, physical properties of alloys, computational approches, etc. You can read and summarize our text from 93 page to 135 page or find other references.

Midterm: 19th April (Tuesday) 7 PM – 9 PM

Scope: text ~ 144 pages/ teaching note ~ #11/ and references